

運輸省港湾技術研究所

港湾技術研究所 報告

REPORT OF
THE PORT AND HARBOUR RESEARCH
INSTITUTE

MINISTRY OF TRANSPORT

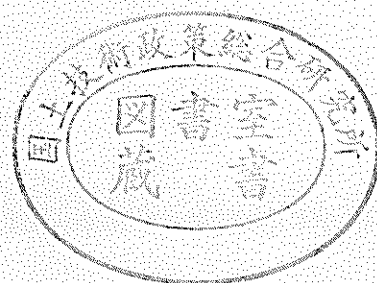
資料係
文献複写
禁持出

VOL. 9

NO. 3

SEPT. 1970

NAGASE, YOKOSUKA, JAPAN



港湾技術研究所報告 (REPORT OF P.H.R.I.)

第9巻 第3号 (Vol. 9, No. 3), 1970年9月 (Sept. 1970)

目 次 (CONTENTS)

1. Numerical Experiments on Wave Statistics with Spectral Simulation
..... Yoshimi GODA..... 3
(波浪の統計的性質に関する数値実験..... 合田良実)
2. 流れの中の風波についての実験的研究 (1) 加藤 始・佐野喜久雄..... 59
(Experimental Study of Wind Waves on Water Currents (1st Report)
..... Hajime KATO and Kikuo SANO)
3. 静的載荷試験による空港舗装の実験的研究
..... 須田 颯・森口 拓・佐藤勝久
吉田富雄・川本晴郎・阿部洋一..... 89
(Experimental Studies on Airport Pavements by Static Loading Tests
..... Hiroshi SUDA, Hiraku MORIGUCHI, Katsuhisa SATO,
Tomio YOSHIDA, Haruo KAWAMOTO and Yoichi ABE)
4. アルミナセメントを使用したプレパックドコンクリートの諸特性について
..... 青木義典・関 博・小野寺幸夫..... 111
(Basic Properties of Prepacked Concrete Using Alumina Cement
..... Yoshinori AOKI, Hiroshi SEKI and Sachio ONODERA)

1. Numerical Experiments on Wave Statistics with Spectral Simulation

Yoshimi GODA*

Synopsis

The analysis of irregular wave action on maritime structures requires information on statistical characteristics of irregular waves which are described with a power spectrum. Though Cartwright and Loguet-Higgins have presented a theory on the maxima of surface elevation, the statistics of wave heights and periods for a spectrum of broad frequency band have remained unclarified. To serve as a solution to the want of synthetic information on the wave statistics, computer simulation of one-dimensional wave profiles has been carried out for twenty four wave spectra of various functional shapes, each with five to ten runs. Power spectra and wave profiles were all non-dimensionalized to produce universal conclusions. Simulated wave profiles were examined for the maxima of surface elevation, crest-to-trough wave heights, zero-up-cross wave heights, correlation between wave height and period, and the run length of wave heights.

The numerical experiments show that the wave heights defined by the zero-up-cross method practically follow the Rayleigh distribution irrespective of the spectral width parameter. This supports the field reports of the fitness of the Rayleigh distribution to the observed records of wind waves. The correlation coefficient between wave heights and periods is found to almost linearly increase with the increase of spectral width parameter. The length of the run of zero-up-cross wave heights is most closely related to the peakedness of a power spectrum. The results of wave simulation with double peaked spectra justify the use of energy concept to estimate the representative height and period of wave system composed of wind waves and swells. In addition, for laboratory simulation of ocean waves with an automatically controlled wave paddle, the number of component waves for the input is recommended to be more than fifty.

* Chief of Wave Laboratory, Hydraulics Division

1. 波浪の統計的性質に関する数値実験

合 田 良 実*

要 旨

港湾や海岸の構造物に対する不規則波の作用を解明するためには、波浪のスペクトル特性から、波高、周期の分布などの統計的性質を推定することが必要になる。波のスペクトルのバンド幅が広い場合については、Cartwright と Longuet-Higgins が波形の極大値の分布を計算しているけれども、波高および周期の分布については十分に調べられていない。そこで、こうした波浪の統計的性質に関する総合的なデータを得るため、電子計算機による波形のシミュレーションを行なった。波のスペクトルとしては24種類のさまざまな形状のものを用い各々5~10回のシミュレーションを行なった。スペクトルおよび波形はすべて無次元化したものを用い、一般的な結論を導けるようにした。こうしてシミュレートした波形について、その極大値、極大極小波高、ゼロアップクロス波高、波高と周期の相関係数、波高の連の長さ、などを解析し、その分布を検討した。

この数値実験の結果によれば、ゼロアップクロス法で定義した波高の分布は、スペクトル幅の値に無関係で、実用上レーリー分布と見なせることが示される。これは現地を観測される風浪の波高分布がほぼレーリー分布に従うことに対応する。また、波高と周期の相関係数は、スペクトル幅の値にほぼ正比例している。ゼロアップクロス法による波高の連の長さについては、スペクトルの尖鋭度に密接に関係していることが示される。さらに、2山型のスペクトルについての計算結果から、うねりと風波が共存する場合の波高と周期の代表値は、エネルギーの重ね合わせ方式で求め得ることを確認した。なお、今回の数値実験によれば、不規則波発生装置で現地波を再現させるためには、入力として50以上の成分波が必要と推定される。

* 水工部 波浪研究室長

CONTENTS

Synopsis	3
1. Introduction	7
2. Review of Statistical Theories on Ocean Waves	9
2.1 Power Spectrum and Gaussian Distribution of Surface Elevation	9
2.2 Distribution of Wave Heights and Periods	11
2.3 Effect of Spectral Width on Wave Statistics	12
2.4 Distribution of the Highest Maximum in a Wave Train	13
2.5 Peakedness of Power Spectrum	15
3. Simulation of Irregular Waves with a Digital Computer	16
3.1 Principle of Wave Simulation	16
3.2 Normalization of Surface Elevation and Wave Spectrum	18
3.3 Model Wave Spectra for Numerical Analysis	19
3.4 Reproducibility of Irregular Waves	23
4. Spectral Width and Maxima of Surface Elevation	25
4.1 Spectral Width Parameter	25
4.2 Distribution of the Maxima of Surface Elevation	27
5. Distribution of Wave Heights and Periods	28
5.1 Heights and Periods of Crest-to-Trough Waves	28
5.2 Zero-up-Cross Wave Heights	30
5.3 Zero-up-Cross Periods	33
5.4 Correlation between Wave Heights and Periods.....	35
6. Lengths of the Run of Wave Heights	38
6.1 Theory of the Length of a Run.....	38
6.2 Observed Lengths of the Run of Wave Heights.....	39
7. Discussion of the Results of Wave Simulation for Practical Application	42
7.1 Number of Component Waves for Laboratory Reproduction of Ocean Waves	42
7.2 Wave Heights and Periods for a Double Peaked Spectrum	44
7.3 Applicability of the Rayleigh Distribution for Wave Heights	46
8. Conclusions	47
References	48
Appendix A: List of Symbols.....	50
Appendix B: Table of the Summary of Simulated Waves.....	52

1. Introduction

Ocean waves have two characters of complexity. The one is irregularity, and the other is non-linearity. Irregularity of ocean waves is readily understood if one goes to shore and looks at waves breaking at beach; the heights and periods of breaking waves differ greatly from wave to wave. The breaking of waves, on the other hand, does demonstrate the non-linear nature of water waves. In case of other types of oscillations such as sound waves, seismic waves, etc., they can increase their intensities without no apparent limit. The non-linear nature of water waves, even before the occurrence of wave breaking, presents difficulty in the analysis of ocean waves with large amplitudes.

To clarify these complex characters of ocean waves, various techniques have been applied. The non-linear character of water waves has been studied analytically and experimentally for waves of finite amplitudes but in a regular train. Wave profiles, particle velocities and accelerations, wave pressures, wave breaking conditions, and other properties of finite amplitude waves are now fairly well understood. Engineers can calculate the properties of finite amplitude waves with reasonable accuracy.

The irregularity of ocean waves has been handled from two directions of approach; one by the representation of irregular waves with significant waves or other mean waves, and the other by the analysis of irregular waves in the form of power spectrum. The technique of spectral analysis has been so effective in clarifying the internal mechanism of ocean waves that a detailed study of the generation, development, and deformation of ocean waves cannot be conducted without the employment of power spectral analysis. The technique, though powerful in understanding the nature of waves, is principally based on the linear theory. Actual waves are presumed as the result of superposition of an infinite number of component waves, the energy of which is proportional to the density of power spectrum at the corresponding frequencies. Theories of non-linear wave spectrum have been presented by several researchers (Hasselmann 1962, Tick 1963, Hamada 1965, etc.), but they are mostly aimed at the understanding of non-linear interaction among component waves. The accomplishments of the study on non-linear, regular waves have not been incorporated in the technique of power spectral analysis of the ocean waves.

From the engineer's point of view, both the irregularity and non-linearity of ocean waves are important in the design of marine structures. The incorporation of both the irregularity and non-linearity in design procedure has been tried for the problems of the sliding of an upright section of composite breakwater by Ito et. al. (1966) and the rate of wave overtopping of sea walls by Tsuruta and Goda (1968), based on the calculation of expected values with the statistical distribution of wave heights. With the presumption that the action of waves on structures can be analysed on the basis of wave by wave approach at least statistically, the non-linear character is estimated with the information on regular waves and the effect of wave irregularity is calculated with the wave height distribution.

In this kind of analysis, a detailed information on the statistical properties of waves is needed. The theoretical distribution for wave heights is the Rayleigh distribution which has been shown by Longuet-Higgins (1952) to be applicable

to ocean waves with narrow band spectra. Field observation data of various sources* generally support the Rayleigh distribution for wave heights defined by the zero-up-cross method despite the fact that most of observed waves has power spectra of broad band. A question may be raised as such: why the Rayleigh distribution derived under the condition of narrow band spectrum holds for the height distribution of waves which are not necessarily of narrow band spectra. As for wave periods, Bretschneider (1959) has proposed an empirical distribution that the squares of wave periods follow the Rayleigh distribution. Though he employs the period distribution as a basis of his wave spectrum, the applicability of the empirical distribution has not been fully examined.

The use of significant wave characteristics is common among engineers. The representation of irregular waves with the significant wave has one advantage that the dimensions of waves are readily grasped by this representation, even though the information on the structure of power spectrum is not given. With proper consideration for wave irregularity, the significant wave characteristics serve as the measure of wave dimensions. If the spectral representation of irregular waves is correlated with the representation with significant waves, the engineers' use of the latter can be encouraged.

The study of wave statistics in connection with the power spectrum of surface elevation has been done with actual wave records. But the field data, though they are the only source that should be referred to, are uncontrolled ones in terms of magnitudes and spectral characteristics. The data can check the validity of a theory on wave statistics, but conclusions are often limited to particular situations. It is difficult to derive from field data general conclusions on the statistical properties of ocean waves and the effect of spectral shapes on wave statistics. On the other hand the establishment of the theory of wave statistics for waves with broad band spectra seems impossible beyond the work of Cartwright and Longuet-Higgins (1956) which has presented the theory on the statistics of maxima but not on wave heights.

At this situation, the numerical analysis with the simulation of wave profiles with given characteristics of power spectra becomes a promising means for the study of wave statistics. A numerical study can employ the data of controlled character in comparison with field data. By varying the characteristics of a power spectrum, their effect on wave statistics can be systematically investigated. Maxima of surface elevation, crest-to-trough wave heights, zero-up-cross wave heights, correlation coefficient between wave height and period, and any other property can be defined, measured, and analysed. Actually, numerical study has been suggested by Cartwright (1963), but to the knowledge of the author only the simulation on the apparent length of wind waves has been undertaken by Ewing (1969).

By this reason, numerical experiments with simulation of wave profiles have been carried out in order to provide answers to the questions on the statistical properties of irregular waves. The subsequent chapters review the existing theories on wave statistics [2.], describe the method of wave simulation employed [3.], present the results of wave simulation [4., 5., and 6.], discuss the results for practical application [7.], and summarize the results of the numerical experiments [8.].

* For example, see Bretschneider (1959), Goodnight and Russel (1963), Collins (1967), Goda and Nagai (1968), etc.

Notation—In this report a wave is defined in two different ways as shown in Fig. 1. The one is called the crest-to-trough wave and the other the zero-up-cross wave. A crest-to-trough wave, denoted with an asterisk, begins at a maximum elevation of wave profile and ends at the next maximum regardless of the position of a maximum. The heights of a crest-to-trough wave is the vertical distance between a maximum elevation and the subsequent minimum elevation; in the example of Fig. 1, the heights of seven crest-to-trough waves are designated with H_1^* to H_7^* . The wave period is the time interval between the successive maxima. On the other hand, a zero-up-cross wave is set in when the surface elevation crosses upward the line of mean elevation and set off when the next zero-up-crossing takes place. Bumps of surface elevation are discarded so long as they do not cross the line of mean elevation. In the example of Fig. 1, the heights of four zero-up-cross waves are designated with H_1 to H_4 . The period of zero-up-cross wave is the time interval between the successive zero-up-cross points.

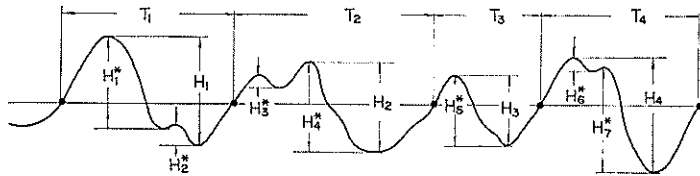


Fig. 1. Definition of wave heights and periods

Other notations used in this report are defined when they first appear and are listed alphabetically in Appendix A.

2. Review of Statistical Theories on Ocean Waves

2.1 Gaussian Distribution and Power Spectrum of Surface Elevation

The random nature of ocean waves is usually described as a stationary Gaussian process. This means two features of ocean waves: the Gaussian distribution of instantaneous surface elevations and the equality of the ensembles with respect to time and space. Thus, a number of the data of surface elevation sampled at a fixed point over a long period of time (or those sampled at an instant over a large area) follow the distribution of

$$p(\eta) = \frac{1}{\sqrt{2\pi} \sigma} \exp[-\eta^2/2\sigma^2], \quad (1)$$

where $\sigma^2 = \overline{\eta^2}$ denotes the variance of surface elevation, η . The zero level of η is taken at the mean surface elevation so that $\overline{\eta} = 0$.

The properties of a statistical distribution can be examined by means of the following moments:

$$\left. \begin{aligned} \mu_1 = \overline{\eta} &= \int_{-\infty}^{\infty} \eta p(\eta) d\eta \\ \mu_k &= \int_{-\infty}^{\infty} (\eta - \overline{\eta})^k p(\eta) d\eta. \end{aligned} \right\} \quad (2)$$

The first moment is the mean, and the second moment gives the variance, σ^2 . The third moment yields the skewness $\sqrt{\beta_1}$ as:

$$\sqrt{\beta_1} = \mu_3 / \mu_2^{3/2}. \quad (3)$$

The fourth moment defines the kurtosis which is a parameter for the peakedness of a statistical distribution as

$$\beta_2 = \mu_4 / \mu_2^2. \quad (4)$$

If the distribution is strictly Gaussian, then $\mu_1 = \mu_3 = 0$ because of symmetry of Eq. 1 with respect to $\eta = 0$. The second moment is σ^2 by definition, and the fourth moment is calculated as $3\sigma^4$. Thus the skewness and kurtosis of the Gaussian distribution become

$$\sqrt{\beta_1} = 0, \quad \text{and} \quad \beta_2 = 3. \quad (5)$$

The Gaussian distribution of surface elevation of ocean waves is an approximation. Detailed examination of wave records reveals a slight deviation from Eq. 1 with a tendency of positive peaks being greater than negative depressions. Kinsman (1964, p. 344) has reported a positive skewness of 0.045 and 0.168, and Goda and Nagai (1968) have obtained the skewness ranging from -0.42 to 1.98 but mostly with positive value. The chi-square test also fails to support the fitness of the Gaussian distribution.

The deviation from the Gaussian distribution is not great, however. Histograms of sampled surface elevation are close to that described by Eq. 1. If the Gaussian distribution is assumed to hold for the surface elevation, waves can be resolved as a sum of infinite number of wavelets with infinitesimal amplitudes and random phases by virtue of the central limit theorem. Thus the surface elevation at a fixed point, $\eta(t)$, is expressed as

$$\eta(t) = \sum_{n=1}^{\infty} a_n \cos(2\pi f_n t + \phi_n), \quad (6)$$

in which a_n denotes the amplitude of the n -th wavelet, f_n the frequency, and ϕ_n the phase. The amplitude a_n is related to the power spectrum (two-sided) $S(f)$ as

$$\sum_f^{f+\delta f} a_n^2 = 4S(f)df. \quad (7)$$

In the form of pseudo-integral representation, the surface elevation is

$$\eta(t) = 2 \int_0^{\infty} \sqrt{S(f)} df \cos(2\pi ft + \phi). \quad (8)$$

These relations afford the basis of wave simulation as will be discussed later.

The variance of the surface elevation, σ^2 , can be calculated from Eq. 6 as

$$\sigma^2 = \lim_{t_0 \rightarrow \infty} \frac{1}{t_0} \int_0^{t_0} \eta^2 dt = 2 \int_0^{\infty} S(f) df. \quad (9)$$

The E -value which appears in the P-N-J method for wave forecasting is twice the variance; hence,

$$E = 2\sigma^2 = 4 \int_0^{\infty} S(f) df. \quad (10)$$

2.2 Distributions of Wave Heights and Periods

The heights of ocean waves, defined by either the crest-to-trough method or the zero-up-cross method, are not uniform but statistically distributed. Longuet-Higgins (1952) has theoretically shown that when the wave spectrum is of narrow frequency band the distribution of η_{\max} is a Rayleigh distribution of the following:

$$p(\eta_{\max})d\eta_{\max} = \frac{\eta_{\max}}{\sigma^2} \exp[-\eta_{\max}^2/2\sigma^2]d\eta_{\max} . \quad (11)$$

The mean value of η_{\max} is obtained from Eq. 11 as

$$\bar{\eta}_{\max} = \int_0^{\infty} \eta_{\max} p(\eta_{\max})d\eta_{\max} = \sqrt{\frac{\pi}{2}} \sigma . \quad (12)$$

In the case of a narrow frequency spectrum, the wave height is twice the maximum of surface elevation, or $H=2\eta_{\max}$. Thus the distribution of wave heights is

$$p(H)dH = \frac{1}{4} \frac{H}{\sigma^2} \exp\left[-\frac{H^2}{8\sigma^2}\right]dH . \quad (13)$$

The above equation can be rewritten with the mean wave height of $\bar{H} = \sqrt{2\pi} \sigma$ as

$$p(H)dH = \frac{\pi}{2} \left(\frac{H}{\bar{H}}\right) \exp\left[-\frac{\pi}{4} \left(\frac{H}{\bar{H}}\right)^2\right] d\left(\frac{H}{\bar{H}}\right) , \quad (14)$$

which is more conventional than Eq. 13.

The average heights of the highest one n -th waves have been numerically calculated by Longuet-Higgins. His results expressed in terms of σ are

$$H_{1/10} = 5.090\sigma , \quad H_{1/3} = 4.004\sigma , \quad \text{and} \quad \bar{H} = \sqrt{2\pi} \sigma = 2.507\sigma . \quad (15)$$

The relations between these heights of mean waves are immediately derived as

$$\frac{H_{1/10}}{H_{1/3}} = 1.27 , \quad \frac{H_{1/3}}{\bar{H}} = 1.60 , \quad \text{and} \quad \frac{\bar{H}}{H_{1/3}} = 0.626 . \quad (16)$$

Longuet-Higgins also gives the expected value of maximum wave height H_{\max} in a sample of N waves. The approximate expression of H_{\max} for large N is

$$\frac{\bar{H}_{\max}}{2\sigma} = \sqrt{2 \ln N} + \frac{\gamma}{\sqrt{2 \ln N}} + O[(\ln N)^{-3/2}] , \quad (17)$$

where γ is Euler's constant, 0.5772. . .

A few more quantities of wave heights can be obtained from Eq. 13. The mode, or the most frequent value, is

$$H_{\text{modo}} = 2\sigma . \quad (18)$$

The root-mean-square wave height is

$$H_{\text{r.m.s.}} = 2\sqrt{2} \sigma = 2.828\sigma . \quad (19)$$

And the standard deviation of wave height from the mean is

$$\sigma(H) = \sqrt{H_{\text{r.m.s.}}^2 - \bar{H}^2} = 1.309\sigma . \quad (20)$$

As for the distribution of wave periods, Bretschneider (1959) assumed a Rayleigh distribution to hold for the square of wave period, T^2 . His expression for the wave period distribution is

$$p(T)dT=2.7\frac{T^3}{\bar{T}^4}\exp\left[-0.675\left(\frac{T}{\bar{T}}\right)^4\right]dT, \quad (21)$$

where \bar{T} denotes the mean wave period. If the wave period follows the above distribution, its standard deviation from the mean is given by

$$\sigma(T)=0.281\bar{T}. \quad (22)$$

2.3 Effect of Spectral Width on Wave Statistics

The distribution of η_{\max} expressed by Eq. 11 has been obtained for waves with a narrow frequency spectrum, which does not necessarily apply for most of ocean waves. For waves with a broad frequency spectrum, Cartwright and Longuet-Higgins (1956) has derived the following statistical distribution for η_{\max} , introducing a spectral width parameter ϵ :

$$p(x)=\frac{1}{\sqrt{2\pi}}\left[\epsilon\exp[-x^2/2\epsilon^2]+\sqrt{1-\epsilon^2}x\exp[-x^2/2]\int_{-\infty}^{x\sqrt{1-\epsilon^2}/\epsilon}\exp[-t^2/2]dt\right], \quad (23)$$

where:

$$x=\eta_{\max}/\sigma, \quad (24)$$

$$\epsilon^2=\frac{m_0m_4-m_2^2}{m_0m_4}, \quad (25)$$

$$m_n=\int_0^\infty S(f)f^n df. \quad (26)$$

The spectral width parameter ϵ has a value between 0 and 1. For the limiting case of $\epsilon \rightarrow 0$ or an infinitely narrow spectrum, Eq. 23 becomes

$$p(x)=\begin{cases} x\exp[-x^2/2], & \text{for } x \geq 0 \\ 0, & \text{for } x < 0, \end{cases} \quad (27)$$

which is the Rayleigh distribution of Eq. 11. For another limiting case of $\epsilon \rightarrow 1$, Eq. 23 is reduced to a Gaussian distribution of

$$p(x)=\frac{1}{\sqrt{2\pi}}\exp[-x^2/2]. \quad (28)$$

In this case, maxima of surface elevation appear below the mean sea level with the equal frequency as those above the mean sea level. For intermediate values of ϵ between 0 and 1, Cartwright and Longuet-Higgins have given graphs of $p(x)$.

The mean and standard deviation of η_{\max} have also been given from the calculation of the moments of $p(x)$ as:

$$\bar{\eta}_{\max}=\sqrt{\frac{\pi}{2}(1-\epsilon^2)}, \quad (29)$$

$$\sigma(\eta_{\max})=\sqrt{1-\left(\frac{\pi}{2}-1\right)(1-\epsilon^2)}.$$

The mean of the maxima of surface elevation decrease as ϵ increases, while the standard deviation increases.

The parameter ϵ which governs the distribution of maxima of surface elevation is calculated by Eq. 25 with the moments of power spectrum. It can also be estimated from the numbers of maxima and zero-up-crossings. According to Rice (1944), the number of maxima N_1 and that of zero-up-crossings N_0 in the record with a duration of L are given by

$$N_1 = \sqrt{m_4/m_2} L, \quad \text{and} \quad N_0 = \sqrt{m_2/m_0} L. \quad (30)$$

Since the ratio N_0/N_1 gives $m_2/\sqrt{m_0 m_4}$, Eq. 25 is rewritten with the relation of Eq. 30 as

$$\epsilon = \sqrt{1 - (N_0/N_1)^2}. \quad (31)$$

The above derivation by Cartwright and Longuet-Higgins is for the maxima of surface elevation and not for the wave heights. They made comments that the statistical distribution of wave amplitude is more difficult to obtain theoretically than that of maxima . . . , but it must in general be different from the Rayleigh distribution. By the wave amplitude they referred to the half distance between a maximum and the succeeding minimum of the surface elevation. They did not give consideration to the wave height defined by the zero-up-cross method. Engineer's experience that the Rayleigh distribution is a good approximation to the statistical distribution of wave heights is explained with the difference in the definition of wave height between engineers and statisticians.

2.4 Distribution of the Highest Maximum in a Wave Train

The highest maximum in a train of a given number of waves is an important problem in engineering. Cartwright and Longuet-Higgins have derived the probability density for the distribution of the highest in the sample of N maxima as:

$$p^*(x_{\max}) = \frac{d}{dx_{\max}} [1 - q(x_{\max})]^N, \quad (32)$$

where $x = \eta_{\max}/\sigma$ as given by Eq. 24 and $q(x)$ is the cumulative distribution of x defined by

$$q(x) = \int_x^{\infty} p(x) dx. \quad (33)$$

Cartwright and Longuet-Higgins have shown an approximate form of $q(x_{\max})$ for large values of N as

$$q(x_{\max}) \doteq \sqrt{1 - \epsilon^2} \exp[-x_{\max}^2/2] + O\left(\frac{1}{x_{\max}^3} \exp[-x_{\max}^2/2\epsilon^2]\right). \quad (34)$$

With the above approximation, the mean value of x_{\max} has been estimated as

$$\frac{\bar{x}_{\max}}{\sqrt{\mu_2'}} \doteq \frac{1}{\sqrt{1 - \frac{1}{2}\epsilon^2}} \left\{ \sqrt{\ln(\sqrt{1 - \epsilon^2} N)} + \frac{1}{2} \frac{\gamma}{\sqrt{\ln(\sqrt{1 - \epsilon^2} N)}} \right\}, \quad (35)$$

where μ_2' is the variance of x and given by

$$\mu_2' = 2 - \epsilon^2 . \quad (36)$$

The number of maxima, N , is related to the number of zero-up-crossings, N_0 , through Eq. 31. Therefore, the mean of x_{\max} is rewritten with Eqs. 35 and 31 as:

$$\bar{x}_{\max} = \sqrt{2 \ln N_0} + \frac{\gamma}{\sqrt{2 \ln N_0}} . \quad (37)$$

The above relation has been derived by Davenport (1964) in the study of the gust loading problem. He has also obtained an explicit form of $p^*(x_{\max})$ for large values of N as follows. The probability that the highest of N maxima has the value between x_{\max} and $x_{\max} + dx_{\max}$ is the probability that one of the maxima has this value and the rest are smaller, i.e.,

$$p^*(x_{\max})dx_{\max} = N[1 - q(x_{\max})]^{N-1} p(x_{\max})dx_{\max} = d[1 - q(x_{\max})]^{N-1} ,$$

which is equivalent to Eq. 32. For large values of N , the following approximation can be made for the term in the right hand side of the above equation:

$$\lim_{N \rightarrow \infty} [1 - q(x_{\max})]^{N-1} = \lim_{N \rightarrow \infty} \left[1 - \frac{\xi}{N} \right]^{N-1} = e^{-\xi} , \quad (38)$$

in which ξ stands for $Nq(x_{\max})$. With the expression of Eq. 34 available for $q(x_{\max})$, ξ is expressed as

$$\xi = Nq(x_{\max}) = N_0 \exp[-x_{\max}^2/2] . \quad (39)$$

With the use of the above asymptotic form, $p^*(x_{\max})$ is rewritten as

$$p^*(x_{\max})dx_{\max} = d[e^{-\xi}] = x_{\max} \xi e^{-\xi} dx_{\max} . \quad (40)$$

In addition to the mean of x_{\max} , Davenport has calculated the mode and standard deviation of x_{\max} as follows:

$$\text{mode}(x_{\max}) = \sqrt{2 \ln N_0} , \quad (41)$$

$$\sigma(x_{\max}) = \frac{\pi}{\sqrt{\sigma}} \frac{1}{\sqrt{2 \ln N_0}} . \quad (42)$$

Thus the highest surface elevation in a wave train is statistically determined by the number of zero-up-crossings N_0 irrespective of the value of the spectral width parameter ϵ .

The largest wave height in a wave train has been studied by Longuet-Higgins (1952) for waves with a narrow frequency spectrum. It is the limiting case of the above calculation with $\epsilon=0$. A wave height is simply twice a maximum of surface elevation. Therefore, equations in the above hold for the amplitude of the largest wave height H_{\max} . When a spectrum has a broad frequency band, H_{\max} is expected to be smaller than $2\eta_{\max}$ since the highest η_{\max} is not necessarily succeeded by the lowest η_{\min} .

2.5 Peakedness of Power Spectrum

In the process of wave simulation and data analysis to be described in the

subsequent chapters, it became evident that the peakedness of a power spectrum plays an important role on the statistics of wave heights defined by the zero-up-cross method. A problem has arisen as to the definition of peakedness of a power spectrum. One possible method is that similar to the kurtosis of Eq. 4. But it yields an extremely large value for the spectra in the form of f^{-5} even though their spectral peaks may not be quite sharp. Another approach is the use of Q employed in the theory of electric circuit; Q is defined as $f_0/(f_1 - f_2)$ where f_0 is the resonant frequency, and f_1 and f_2 are such that the amplitude of resonant curve at these frequencies is $1/\sqrt{2}$ of the resonant peak. But in the practice of wave spectral analysis, a peak of a wave spectrum is difficult to determine accurately; sometimes a wave spectrum has two or more peaks.

A third possibility is found in the treatment by Tucker (1963), who introduced the following quantity ϕ as a measure of "peakiness" of a wave spectrum:

$$\phi = \frac{\int_0^{\infty} E(f)^2 df}{\left[\int_0^{\infty} E(f) df \right]^2}, \quad (43)$$

where $E(f)$ is the energy spectrum of waves. According to Tucker, ϕ controls the random error in the measurement of the root-mean-square value of wave height, and its value is typically of the order of ten for locally generated waves but may be as high as 100 for swell from a distant storm. The quantity ϕ defined by Eq. 43 has a dimension of time, although a non-dimensional quantity is preferable as a general parameter.

After these considerations, the following quantity Q_p has been selected as a measure of the peakedness of a wave spectrum:

$$Q_p = \frac{2 \int_0^{\infty} f S(f)^2 df}{\left[\int_0^{\infty} S(f) df \right]^2}. \quad (44)$$

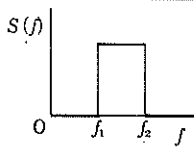
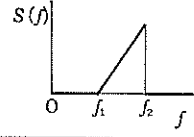
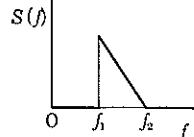
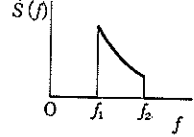
A few examples of the value of Q_p are shown in Table 1.

The spectral peakedness parameter Q_p is somewhat related to the spectral width parameter ϵ , but it is not a simple function of ϵ . Figure 2 shows the correlation of Q_p and ϵ of the model wave spectra employed in the present simulation analysis (see 3.3 for details of the spectra). A small value of ϵ is associated with a large value of Q_p , but the value of ϵ around 0.7 is associated with the value of Q_p ranging from 0.9 to 3.0. For a spectrum with a single peak at $f = f_0$, Q_p may be roughly estimated by

$$Q_p \approx 2f_0/(f_1 - f_2), \quad (45)$$

where f_1 and f_2 are such frequencies at which $S(f_1) = S(f_2) = \frac{1}{5} S(f_0)$.

Table 1. Examples of Spectral Peakedness, Q_p

No.	Power Spectral	Spectral Peakedness
I	 $S(f) = \begin{cases} 1 & (f_1 \leq f \leq f_2) \\ 0 & (f < f_1, f > f_2) \end{cases}$	$Q_p = \frac{f_2 + f_1}{f_2 - f_1}$
II	 $S(f) = \begin{cases} f - f_1 & (f_1 \leq f \leq f_2) \\ 0 & (f < f_1, f > f_2) \end{cases}$	$Q_p = \frac{2}{3} \left(4 \frac{f_2}{f_2 - f_1} - 1 \right)$
III	 $S(f) = \begin{cases} f_2 - f & (f_1 \leq f \leq f_2) \\ 0 & (f < f_1, f > f_2) \end{cases}$	$Q_p = \frac{2}{3} \left(4 \frac{f_2}{f_2 - f_1} - 3 \right)$
IV	 $S(f) = \begin{cases} f^{-n} & (f_1 \leq f \leq f_2) \\ 0 & (f < f_1, f > f_2) \end{cases}$	$Q_p = (n-1) \frac{1 - \left(\frac{f_1}{f_2}\right)^{2(n-1)}}{\left[1 - \left(\frac{f_1}{f_2}\right)^{n-1}\right]^2}$

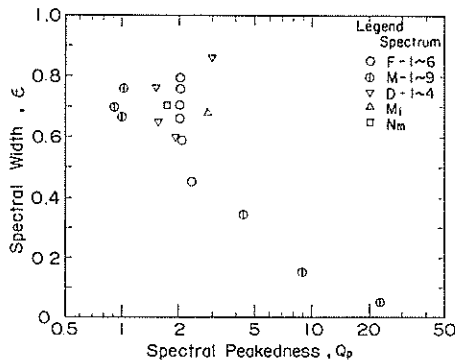


Fig. 2. Correlation between the spectral width parameter and peakedness parameter

3. Simulation of Irregular Waves with a Digital Computer

3.1 Principles of Wave Simulation

(1) Fundamental equation

The simulation of $\eta(t)$ with a digital computer can be carried out in two different ways (Borgman 1969). The one method employs a pure random signal such as the white noise and modifies it through a transformation function selected for specific spectral characteristics. The method has been employed by Hino (1967) for the test of his wave prediction filter. Borgman (1969) has also demon-

strated its effective use for the wave simulation with directional power spectra. The other method is based on Eq. 8, which is to be rewritten in the form of summation as

$$\eta(t) = \lim_{K \rightarrow \infty} \sum_{i=1}^K A_i \cos(2\pi f_i t + \phi_i) \quad (46)$$

with

$$A_i = 2\sqrt{S(f_i)\Delta f_i} .$$

The latter method is simple and straight forward. Though the computation by the latter is time-consuming, it has the advantage that no restriction is imposed on functional shape of $S(f)$. Since the simulation with various power spectra was scheduled as seen in 3.3, Eq. 46 was employed in this report for the computation of wave profiles.

(2) Determination of component frequencies

The component frequencies $f_1, f_2, f_3, \dots, f_K$ are required to be non-correlating so that they will not constitute harmonics each other. At the same time, it is desirable that the amplitudes of component waves will be approximately equal in magnitude. Since the spectral function can take various shapes, the realization of the latter requirement is in general difficult.

The selection of frequency was done in the following way. First, the range of frequency from the lowest, f_{\min} , to the highest, f_{\max} , was divided into $(K-1)$ sub-ranges with the deviding frequencies constituting a power series of

$$\left. \begin{aligned} f_1' &= f_{\min} + \frac{f_{\max} - f_{\min}}{K-1} \\ f_2' &= f_1' \times C_K, \dots, \quad f_i' = f_{i-1}' \times C_K, \dots \\ f_{K-1}' &= f_1' \times C_K^{K-2} \end{aligned} \right\} \quad (47)$$

where: $C_K = \left[\frac{f_{\max}}{f_1'} \right]^{1/(K-2)}$.

Then, the secondary deviding frequencies $f_1'', f_2'', f_3'', \dots, f_{K-1}''$ were chosen at random in respective sub-ranges. The initial frequency f_0'' was set equal to f_{\min} and the last one was $f_K'' = f_{\max}$. The selection was done with the aid of a random-number-generation process programed on the computer. Finally the component frequency f_i and its band width Δf_i were calculated as

$$\left. \begin{aligned} f_i &= \frac{1}{2}(f_{i-1}'' + f_i'') \\ \Delta f_i &= f_i'' - f_{i-1}'' \end{aligned} \right\} \quad i=1, 2, \dots, K. \quad (47)$$

The above process of random selection of component frequency was repeated for each run of each wave spectrum.

(3) Determination of the phase of a component wave

The phase ϕ_i must be chosen at random in order that the resultant function $\eta(t)$ would follow the Gaussian distribution. This has been done with the generation of random numbers equally distributed between 0 and 2π . The randomness of the phase thus determined has been verified by Suzuki (1969). Like the com-

ponent frequency by this process, the random selection of component phase was repeated for each run of each wave spectrum.

(4) Number of component waves

The number of component waves, K , is required as large as feasible in order that the Gaussian distribution of $\eta(t)$ would be realized asymptotically. But an increase in K directly expands the computation time. Preliminary investigations showed that the number of $K=200$ would be sufficiently large to simulate random surface elevation for the standard spectrum of ocean waves. The performance of the computer available, however, was not fast enough to allow the employment of 200 component waves for the intended number of simulation runs necessary for statistical analysis. The asymptotic approach to the Gaussian distribution was found slow for the number of component waves over about fifty. And the deviation from the Gaussian was noticeable only at the highest maximum of wave profile (see 7.1). A compromise was made in this study between the computation time and the realization of the Gaussian distribution, and most of the runs were carried out with 50 component waves for single peaked spectra and with 60 component waves for double peaked spectra.

(5) Length of time step

The computation of wave profile by Eq. 46 is done at discrete intervals. The time interval Δt was set to satisfy the condition of

$$\Delta t \leq \frac{1}{5f_{\max}}. \quad (49)$$

In the measurement of power spectrum, the condition for the time interval of data sampling is

$$\Delta t < \frac{1}{2f_{\max}}. \quad (50)$$

The stricter condition of Eq. 49 was employed in this study after preliminary tests in order to ensure few overlooking of maxima and minima of surface elevation.

(6) Duration of simulated wave record

The length of a simulated wave record was controlled so that 200 zero-up-cross waves would be generated in one run. The number of data under the condition of Eq. 49 varied from about 1000 to 6000 depending upon the highest frequency f_{\max} and the spectral width parameter ϵ .

3.2 Normalization of Wave Profile and Spectrum

Though actual wave records are obtained with the dimension of length for surface elevation and that of time for duration, some kind of normalization for a wave record is preferable for the study of wave statistics, especially in this kind of numerical experiments. The standard quantity of reference for the normalization of surface elevation will be the root-mean-square value of $\eta(t)$, or σ given by Eq. 9. This value is calculated for the surface elevation to be computed by Eq. 46 as

$$\sigma^2 = \frac{1}{2} \sum_{i=1}^K A_i^2 = 2 \sum_{i=1}^K S(f_i) \Delta f_i. \quad (51)$$

The surface elevation $\eta(t)$ and the amplitude of component wave A_i are divided by σ given in the above.

As for the normalization of time and frequency, the frequency at which a power spectrum shows the maximum density, f_0 , has been taken as the reference quantity. Therefore, the fundamental equation for the computation of surface elevation is rewritten in normalized form as

$$\eta(t) = \sum_{i=1}^K A_i \cos(2\pi f_i t + \phi_i), \quad (52)$$

where:

$$\left. \begin{aligned} \eta(t) &= \eta(f_0 t) / \sigma \\ A_i &= A_i / \sigma = 2\sqrt{S(f_i) \Delta f_i} / \sigma \\ f_i &= f_i / f_0 \\ t &= f_0 t \end{aligned} \right\} \quad (53)$$

Under this normalization, the normalized surface elevation has the root-mean-square of unit value, i.e.,

$$\sigma = 1. \quad (54)$$

The integral of the power spectrum of the normalized surface elevation has the value of $\frac{1}{2}$. In the form of summation, it is expressed as

$$\sum_{i=1}^K S(f_i) \Delta f_i = \frac{1}{2}, \quad (55)$$

in which $S(f_i)$ denotes the normalized power spectrum.

In the subsequent paragraphs all the quantities appear in normalized forms unless otherwise stated. They will be denoted by symbols in standard italic faces since there will be no confusion.

3.3 Model Wave Spectra for Numerical Analysis

Various theoretical spectra of ocean waves have been proposed by Neumann (1953), Bretschneider (1959), Pierson and Moskowitz (1964), Mitsuyasu (1968), and other investigators. Most of wave spectra in the dimensional form are of the power-exponential type of

$$S(f) = A f^{-m} \exp[-B f^{-n}]. \quad (56)$$

For example, Neumann's spectrum corresponds to the case of $m=6$ and $n=2$, and Pierson and Moskowitz's one as well as Bretschneider's one for zero correlation between wave height and period are represented with Eq. 56 with the values of $m=5$ and $n=4$. According to Bretschneider (1963), the spectrum of Eq. 56 can be rewritten as follows:

$$S(f) = (A f_0^{-m}) \left(\frac{f}{f_0}\right)^{-m} \exp\left[-\frac{m}{n} \left(\frac{f}{f_0}\right)^{-n}\right], \quad (57)$$

in which f_0 is the frequency at the maximum spectral density and is given by

$$f_0 = \left(\frac{m}{nB} \right)^{-1/n}. \quad (58)$$

Equation 57 is already in normalized form with respect to frequency. By employing the notation of $f=f/f_0$, it is expressed as

$$S(f) = A' f^{-m} \exp \left[-\frac{m}{n} f^{-n} \right]. \quad (59)$$

The above spectral function has its maximum value at $f=1$, or $f_0=1$. The quantity A' is determined so as to satisfy the normalization condition of Eq. 55. In the practice of numerical computation, the integral of the power spectrum is first evaluated with A' being set to 1 and the result is employed to determine the value of A' by Eq. 55.

The model wave spectra for the numerical analysis of wave statistics have been selected so as to cover broad variations in spectral shape. They have been assigned to clarify the following problems:

- i) The effect of the cut-off frequency in high frequency part of a wave spectrum on wave statistics.
- ii) The effect of the spectral peakedness on wave statistics.
- iii) Differences in the statistics of waves with various, theoretical wave spectra.
- iv) Characteristics of waves simulated with a few number of component waves.
- v) The statistics of waves with a double peaked spectrum such as formed by a superposition of local wind waves and swell from a remote source.

The first problem was investigated for Pierson and Moskowitz's spectrum with $m=5$ and $n=4$ in Eq. 59; the cut-off frequency was varied from 2 to 10. The model spectra for this problem are denoted by F-1 to F-6. The second problem was investigated with the model spectra for which the value of m ranged from 0.5 to 50* while the ratio of n/m being kept at 0.8. The range of frequency varied depending upon the value of m , but the cut-off frequency was determined not to exceed $f_{\max}=5$. The model spectra for the second problem are denoted by M-1 to M-9. The functional shapes of the M-series spectra as well as F-4 spectrum are shown in Fig. 3. As for the theoretical spectra to be compared in the third problem, Neumann's spectrum denoted by N_m and Mitsuyasu's one denoted by M_i were selected. The spectrum M_i employed in this study is

$$S(f) = \begin{cases} A' f^{-5} \exp [f-1], & \text{for } 0.3 \leq f < 1 \\ A' f^{-5}, & \text{for } 1 \leq f < 5 \\ 0, & \text{for } f < 0.3, \text{ or } f > 5, \end{cases} \quad (60)$$

where the quantity A' is determined in the same way as that in Eq. 59. Figure 4 shows the functional shapes of N_m and M_i spectra as well as F-4 spectrum. It is seen that Mitsuyasu's spectrum has a peak sharper than Neumann's one or Pierson and Moskowitz's one.

The fourth problem of the wave simulation with a few component waves was investigated for the spectrum with $m=5$ and $n=4$. The number of component

* A swell from a remote source has a spectrum more peaked than that of wind waves; the value of m reaches 10 in certain occasions.

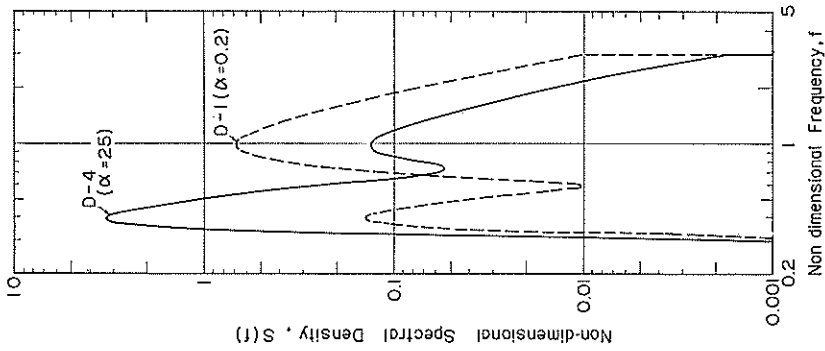


Fig. 3. Shapes of model wave spectra (1)

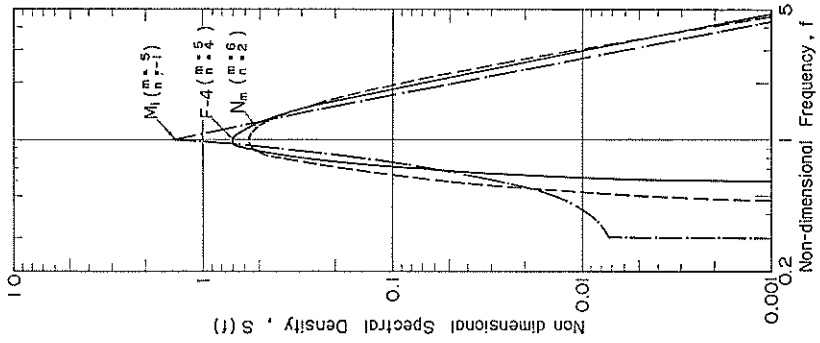


Fig. 4. Shapes of model wave spectra (2)

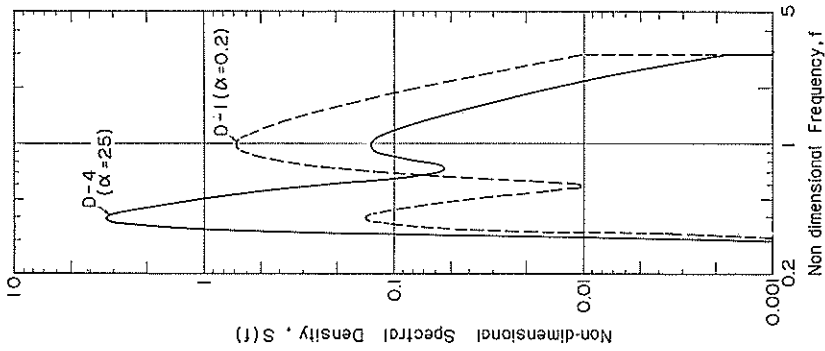


Fig. 5. Shapes of model wave spectra (3)

waves varied from 3 to 10. The model spectra are denoted by K-1 to K-3. This problem is related to the design of an irregular wave generator for laboratory simulation of ocean waves. The last problem of double peaked wave spectra was investigated with the following model wave spectra:

$$S(f) = A' \left\{ \alpha(\beta f)^{-m'} \exp \left[-\frac{m'}{n'} [(\beta f)^{-n'} - 1] \right] + f^{-m} \exp \left[\frac{m}{n} (f^{-n} - 1) \right] \right\}, \quad (61)$$

in which the relative position of low frequency peak β and exponents m , m' , n , and n' were assigned the values of

$$m=5, \quad m'=10, \quad n=4, \quad n'=8, \quad \text{and} \quad \beta=0.4. \quad (62)$$

The factor α which represents the relative magnitude of low frequency peak compared to the high frequency peak was assigned the value of 0.2 to 25. The spectra are denoted by D-1 to D-4, among which the spectra D-1 and D-4 are shown in Fig. 5.

Characteristics of these model wave spectra are summarized in Table 2. The mean frequency, \bar{f} , has been calculated with the first moment of power spectrum defined by Eq. 26 as

$$\bar{f} = m_1/m_0. \quad (63)$$

Table 2. Characteristics of Model Wave Spectra

Spectrum	$\frac{m}{(m')}$	$\frac{n}{(n')}$	$f_{\min} \sim f_{\max}$	K	Nos. of run	ϵ	Q_p	\bar{f}	Remarks
F-1	5.0	4.0	0.5 ~ 2.0	50	5	0.45	2.31	1.18	
F-2	5.0	4.0	0.5 ~ 3.0	50	5	0.59	2.06	1.25	
F-3	5.0	4.0	0.5 ~ 4.0	50	5	0.65	2.02	1.28	
F-4	5.0	4.0	0.5 ~ 5.0	50	10	0.71	2.01	1.29	
F-5	5.0	4.0	0.5 ~ 7.0	50	5	0.76	2.00	1.29	
F-6	5.0	4.0	0.5 ~ 10.0	50	5	0.80	2.00	1.29	
K-1	5.0	4.0	0.7 ~ 2.0	3	9	0.45	2.14	1.16	
K-2	5.0	4.0	0.6 ~ 3.0	5	9	0.60	1.95	1.25	
K-3	5.0	4.0	0.5 ~ 5.0	10	10	0.71	1.91	1.30	
M-1	50.0	40.0	0.95 ~ 1.25	50	10	0.06	22.6	1.01	$(N_0=400 \text{ waves})$
M-2	50.0	40.0	0.95 ~ 1.25	50	10	0.06	22.6	1.01	
M-3	50.0	40.0	0.95 ~ 1.25	100	9	0.06	22.6	1.01	
M-4	20.0	16.0	0.8 ~ 1.8	100	5	0.15	8.89	1.04	
M-5	20.0	16.0	0.8 ~ 1.8	50	10	0.15	8.89	1.04	
M-6	10.0	8.0	0.75 ~ 3.0	50	10	0.34	4.30	1.09	
M-7	2.5	2.0	0.2 ~ 5.0	50	10	0.76	1.04	1.80	
M-8	1.25	1.0	0.15 ~ 5.0	50	10	0.70	0.92	2.28	
M-9	0.5	0.4	0.0 ~ 5.0	50	10	0.67	0.99	2.48	
M_i	5.0	-1.0	0.3 ~ 5.0	50	10	0.68	2.83	1.21	
N_m	6.0	2.0	0.4 ~ 5.0	50	10	0.70	1.70	1.30	
D-1	5.0 (10.0)	4.0 (8.0)	0.3 ~ 3.0	60	10	0.60	1.92	1.22	$\alpha=0.2, \beta=0.4$
D-2	5.0 (10.0)	4.0 (8.0)	0.3 ~ 3.0	60	10	0.65	1.57	1.13	$\alpha=1.0, \beta=0.4$
D-3	5.0 (10.0)	4.0 (8.0)	0.3 ~ 3.0	60	10	0.77	1.56	0.86	$\alpha=5.0, \beta=0.4$
D-4	5.0 (10.0)	4.0 (8.0)	0.3 ~ 3.0	60	10	0.86	2.98	0.58	$\alpha=25.0, \beta=0.4$

Details of spectral characteristics and wave statistics are listed in the table in the Appendix B.

3.4 Reproducibility of Irregular Waves

An example of simulated wave profile is shown in Fig. 6. This is a part of long record of wave simulation with the spectrum F-4 of $m=5$, $n=4$, and $f_{\max}=5.0$. Irregularity in wave profile is readily observed. The power spectrum of the simulated wave record which contains the part shown in Fig. 6 has been obtained for the data of 2000 with the maximum lag of 100 and $\Delta t=0.04$. The result of spectral analysis is compared with the input spectrum in Fig. 7; the input is shown with a solid line while the output is shown with a dashed line connecting open circles. Since the power spectrum has been approximated with a finite number ($K=50$ for this case) of component waves, the input spectrum is represented with a step-wise function. Except for the low frequency zone which belongs to the noise range, the agreement between the input and output spectra is excellent.

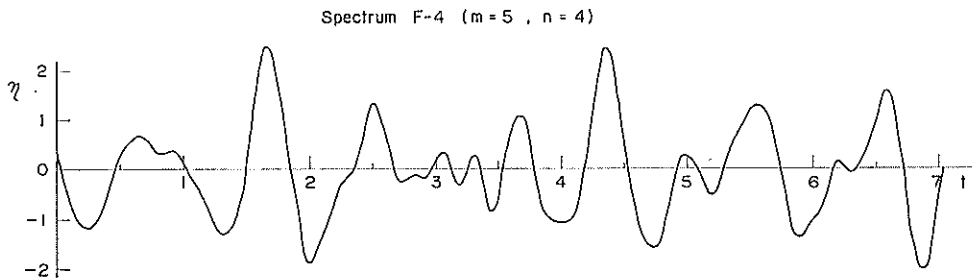


Fig. 6. Example of simulated, non-dimensional wave profile

As for the statistical examination of simulated waves, the following characteristics were investigated:

- i) the Gaussian distribution of surface elevation,
- ii) the skewness of surface elevation, and
- iii) the kurtosis of surface elevation.

Figure 8 shows an example of the distribution of surface elevation. The wave record is the one employed in Figs. 6 and 7. The ranges of surface elevation were so divided that the equal percentage of appearance would be obtained under the Gaussian distribution law. The chi-square value for the 20 divisions was 16.3 for the fitness test of the Gaussian distribution. Since the probability that the chi-square value exceeds this value is about 0.7, the Gaussian distribution can be accepted. The examination of the Gaussian distribution was conducted in the stage of preliminary test with satisfactory results; hence the detailed examination for all of the runs was not undertaken.

The examination of the skewness and kurtosis, however, has been conducted for all the runs. Since the spectral representation of irregular waves presumes the linear summation of infinitesimal component waves and the present simulation is based on the linear process, the skewness of simulated wave profiles should be 0. The observed value of the skewness of each run varied from -0.18 to 0.14 , but it varied at random without any correlation with the spectral width parameter ϵ . The overall average and standard deviation of the skewness of 187 runs have been calculated as

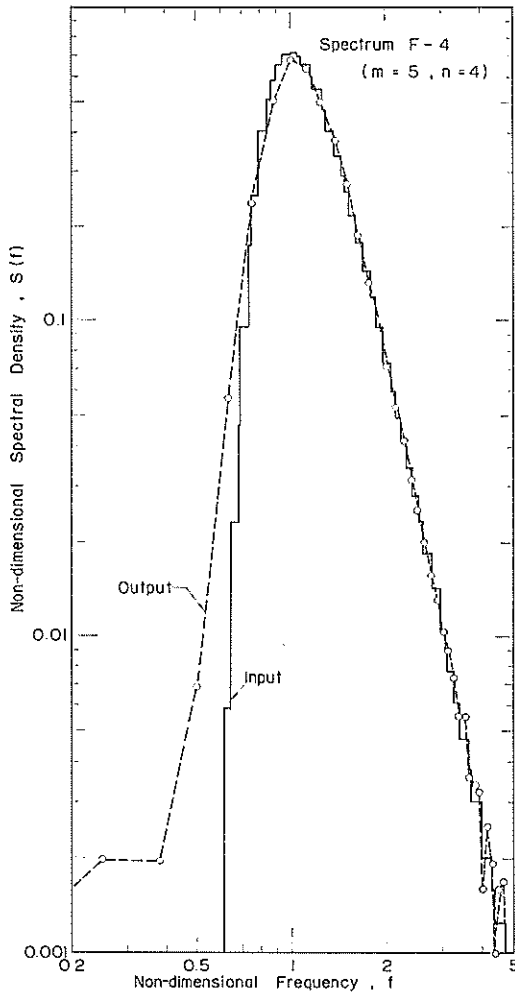


Fig. 7. Comparison of input and output wave spectra

$$\sqrt{\beta_1} = 0.004 \pm 0.051 . \quad (64)$$

The result supports the presumption of zero skewness for the population of simulated wave data.

The theoretical value of the kurtosis for the data following the Gaussian distribution is $\beta_2=3.0$ as shown by Eq. 5. On the other hand if the distribution is uniform between $|\eta| \leq 1$, then the kurtosis becomes $9/5$. If the wave profile is a sinusoid, the kurtosis is calculated as 1.5. The observed value of the kurtosis varied at random from 2.40 to 3.53 without any correlation with the spectral width parameter ϵ , except for the *K*-series spectra. The overall average and standard deviation of the kurtosis of 157 runs excluding the *K*-series spectra have been calculated as

$$\beta_2 = 2.900 \pm 0.204 . \quad (65)$$

Thus the simulated wave records have the kurtosis almost the same with that of the Gaussian distribution. The difference of 0.1 between the average value of simulated waves and the theoretical value of the Gaussian distribution seems to have been produced by the limit in the number of component waves in the simulation, because the *K*-series

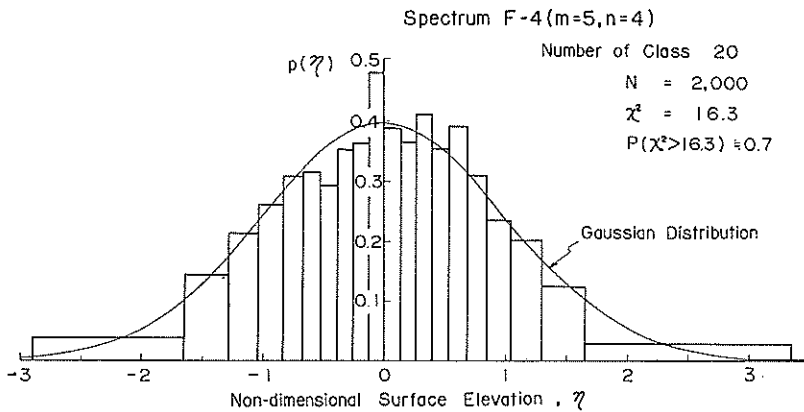


Fig. 8. Example of the distribution of surface elevation

spectra simulated with a few number of component waves show much lower values of the kurtosis than other spectra; this will be discussed in 7.1.

4. Spectral Width and Maxima of Surface Elevation

4.1 Spectral Width Parameter

The spectral width parameter is calculated from the input wave spectra by Eq. 25 and denoted by ϵ_{spec} . It is also obtained from the numbers of zero-up-crossings and maxima of surface elevation by Eq. 31 and denoted by ϵ_{nos} . Two estimations of ϵ averaged for five to ten runs of each spectrum are compared in Fig. 9, which shows little difference between them for the range of ϵ_{nos} from 0.03

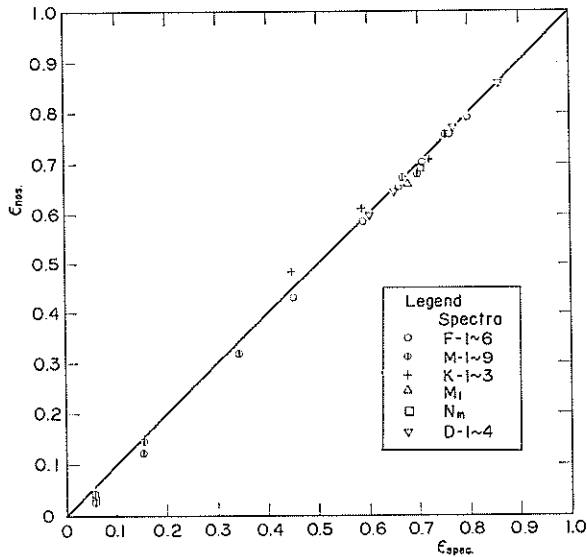


Fig. 9. Comparison of spectral width parameter, ϵ_{nos} and ϵ_{spec}

to 0.86. The agreement suggests the accuracy of Eq. 30 for the estimation of N_0 and N_1 . In fact, the examination of the observed numbers of zero-up-crossings and maxima for 187 runs has yielded the following averages and standard deviations for the ratios between the observed and estimated numbers:

$$\left. \begin{aligned} \frac{(N_0)_{\text{obs}}}{(N_0)_{\text{est}}} &= 0.9985 \pm 0.0212 \\ \frac{(N_1)_{\text{obs}}}{(N_1)_{\text{est}}} &= 0.9934 \pm 0.0187. \end{aligned} \right\} \quad (66)$$

It should be mentioned that the above results were obtained by the sampling of wave profile at the time interval of $\Delta t \leq 1/(5f_{\text{max}})$. When the time interval was chosen at $\Delta t = 1/(2.5f_{\text{max}})$ in the preliminary tests for wave spectra of f^{-5} type, some of maxima of the surface elevation were overlooked and the numbers of maxima were less than those predicted by Eq. 30. This implies that the calculation of the spectral width parameter ϵ from a wave spectrum is to be made in the frequency range of $f=0$ to $f_{\text{max}} \doteq 1/(5\Delta t)$, not to Nuiquist frequency of $f_N = 1/(2\Delta t)$, especially for wind waves with power spectra of f^{-5} type.

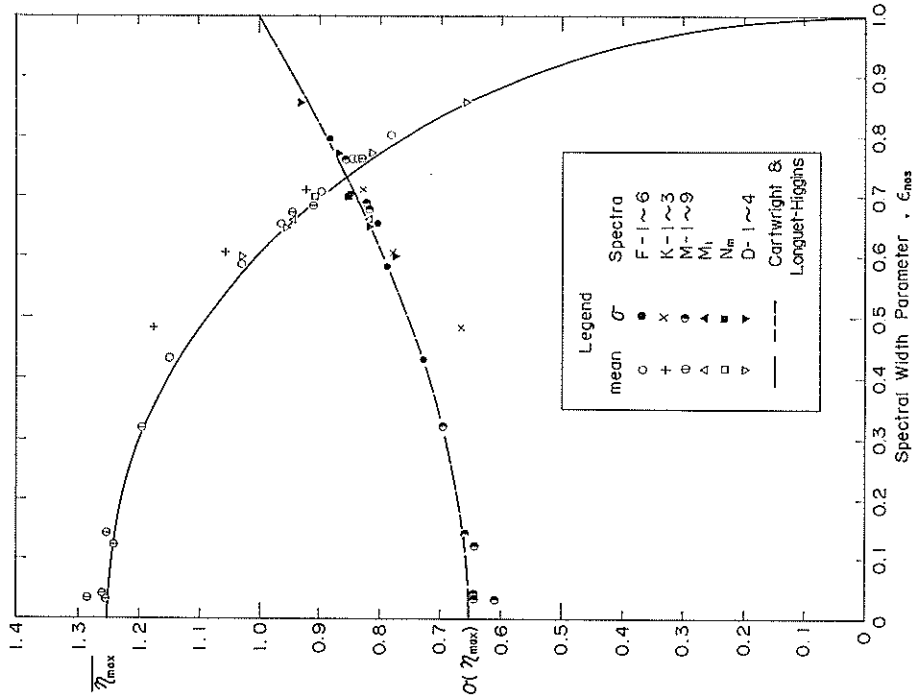


Fig. 11. Mean and standard deviation of the maxima of surface elevation

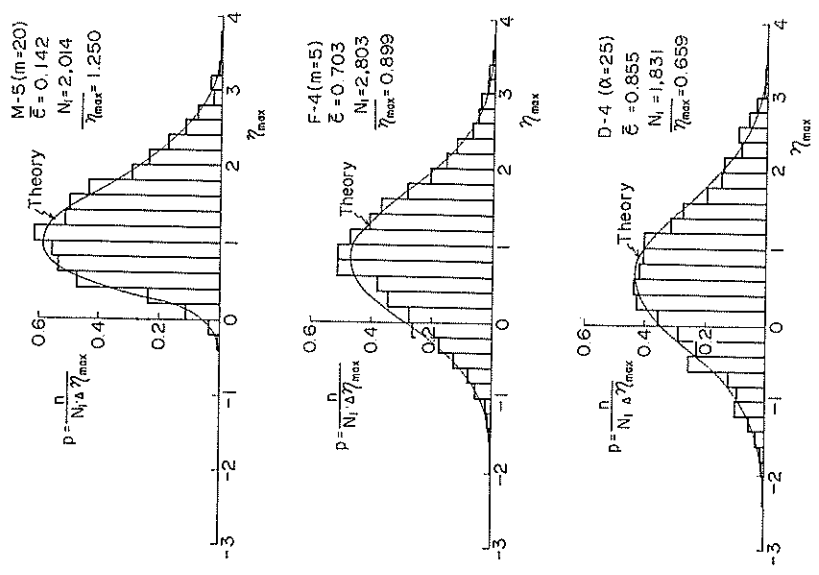


Fig. 10. Examples of the distribution of the maxima of surface elevation

4.2 Distribution of the Maxima of Surface Elevation

The distribution of the maxima of surface elevation is shown in Fig. 10 for model spectra of M-5, F-4, and D-4. Data of five to ten runs for each spectrum are summed up to yield average values for respective ranges of surface elevation. The theoretical distribution of Eq. 23 fits quite well to the observed ones. Another verification of the theoretical distribution is seen in Fig. 11, which shows the mean and standard deviation of η_{\max} for each wave spectrum against the spectral width parameter. Except for the *K*-series spectra simulated with a few numbers of component waves, the theoretical relations of Eq. 29 agree well with the observed values. Therefore, it is concluded that the theory of Cartwright and Longuet-Higgins (1956) quite accurately predicts the general distribution of the maxima of surface elevation, so long as it follows the Gaussian distribution.

The distribution of the highest maximum was examined for the model spectra of F-1 to F-6 with total runs of 35. Figure 12 shows the distribution of $(\eta_{\max})_{\max}$

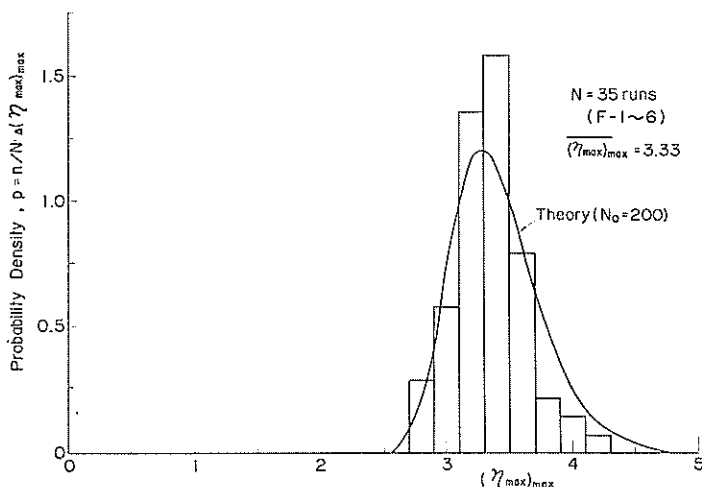


Fig. 12. Histogram of highest maxima in trains of 200 waves

for the 35 runs. An observed number of $(\eta_{\max})_{\max}$ in a specific range with the increment of $\Delta(\eta_{\max})_{\max}$ was divided by $N \cdot \Delta(\eta_{\max})_{\max}$ to give the density of observation. The observed value of $(\eta_{\max})_{\max}$ varied from 2.78 to 4.30 with the mean of 3.33. The theoretical mean for wave trains with 200 zero-up-crossings is calculated as 3.43 by Eq. 37; the mean of 3.33 corresponds to the zero-up-crossings of about 140. The observed distribution of $(\eta_{\max})_{\max}$ is in fair agreement with the theoretical one with $N_0=200$, though the observed one is concentrated in a narrower range than the theoretical one. Slight differences in the mean and distribution seem to be caused by the limit in the number of component waves employed in the simulation.

The highest maxima were also examined for other model spectra. The mean value of $(\eta_{\max})_{\max}$ for five to ten runs of each spectrum has been calculated and is plotted in Fig. 13 against the spectral peakedness Q_p introduced in 2.5. A lowest minimum, $(\eta_{\min})_{\min}$, was regarded as another realization of $(\eta_{\max})_{\max}$ in the negative side, and its absolute value was averaged with $(\eta_{\max})_{\max}$ so as to increase the number of data. The mean value of $(\eta_{\max})_{\max}$ shows a tendency to

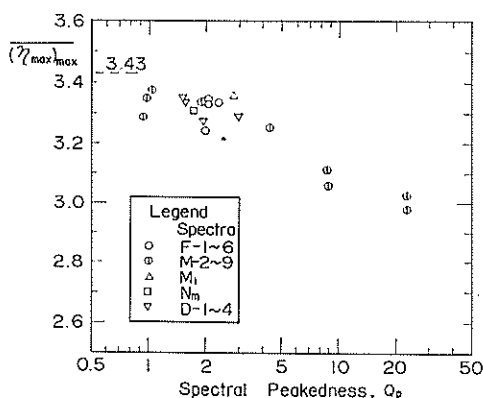


Fig. 13. Mean of the highest maxima of surface elevation in tarins of 200 waves

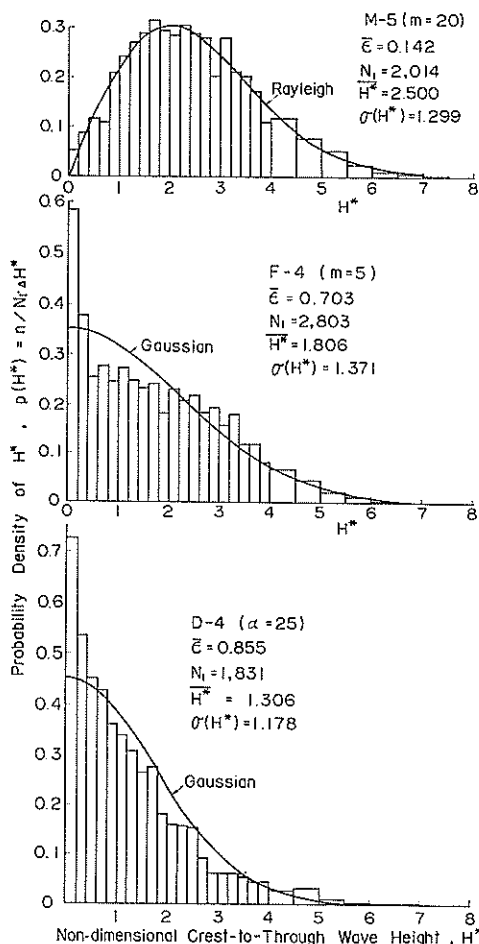


Fig. 14. Examples of the distribution of crest-to-trough wave heights

decrease as Q_p increases. The cause of decrease is not clear. An increase in the number of component waves from 50 to 100 for the spectra M-2 and M-4 with very sharp peaks has not increased the mean value of $(\eta_{max})_{max}$. But it is shown in 6.2 that the average length of the run of wave heights increases as Q_p increases. While the theory concerns with the data of N maxima sampled at random from a great number of maxima, the present data are composed of N continuous maxima which may have a high level of auto-correlation especially when Q_p is large. This auto-correlation of η_{max} for waves with a sharp spectral peak seems to make the value of $(\eta_{max})_{max}$ lower than the theoretical value of Eq. 37.

5. Distribution of Wave Heights and Periods

5.1 Heights and Periods of Crest-to-Trough Waves

Examples of the distribution of crest-to-trough wave heights are shown in Fig. 14. For the model spectrum of M-5 with $\bar{\epsilon}=0.142$, the Rayleigh distribution is a good approximation. On the other hand the model spectra of F-4 with $\bar{\epsilon}=0.703$ and that of D-4 with $\bar{\epsilon}=0.855$ show the distributions somewhat similar to the Gaussian but with intensive concentration at $H^*=0$.

The mean and standard deviation of H^* for each wave spectrum are shown in Fig. 15 against ϵ . Since the mean of crest-to-trough wave heights is twice that of the maxima of surface elevation, i.e. $\bar{H}^*=2\bar{\eta}_{max}$, it follows the theoretical relation of $\bar{H}^*=\sqrt{2\pi(1-\epsilon^2)}$. The standard deviation, however, is not a simple function of ϵ , showing some scatter in the range from 1.1 to 1.4.

The distribution of crest-to-trough

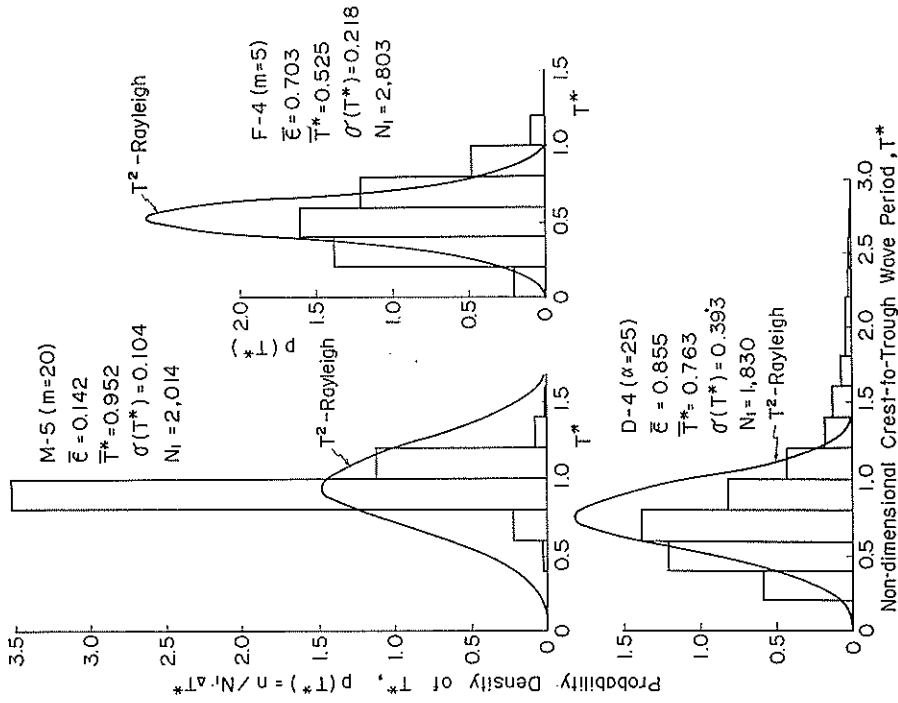


Fig. 16. Examples of the distribution of non-dimensional crest-to-trough wave periods

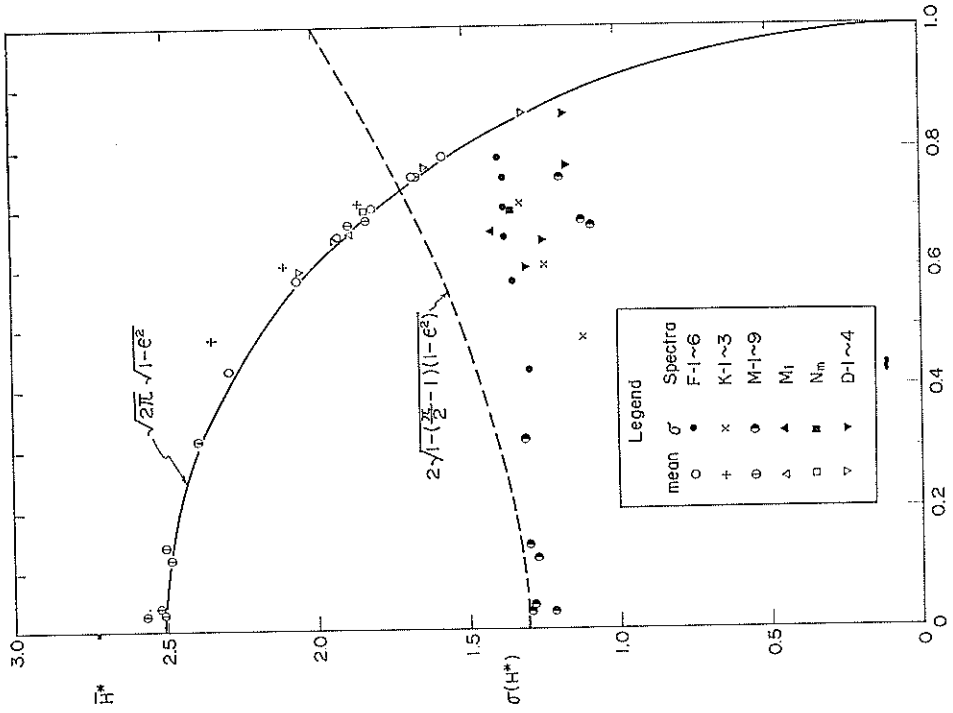


Fig. 15. Mean and standard deviation of non-dimensional crest-to-trough wave heights

wave periods, T^* , are compared with the Rayleigh-type distribution of Eq. 21 in Fig. 16 for the model spectra of M-5, F-4, and D-4. Some of observed distribution (M-5) is narrower than that of Eq. 21, while others (F-4 and D-4) show broader distributions. Thus, the Rayleigh-type distribution of Eq. 21 is not applicable to the distribution of crest-to-trough wave periods in general.

The mean and standard deviation of crest-to-trough wave periods are found to be functions of the spectral width parameter ϵ as shown in Fig. 17. The mean

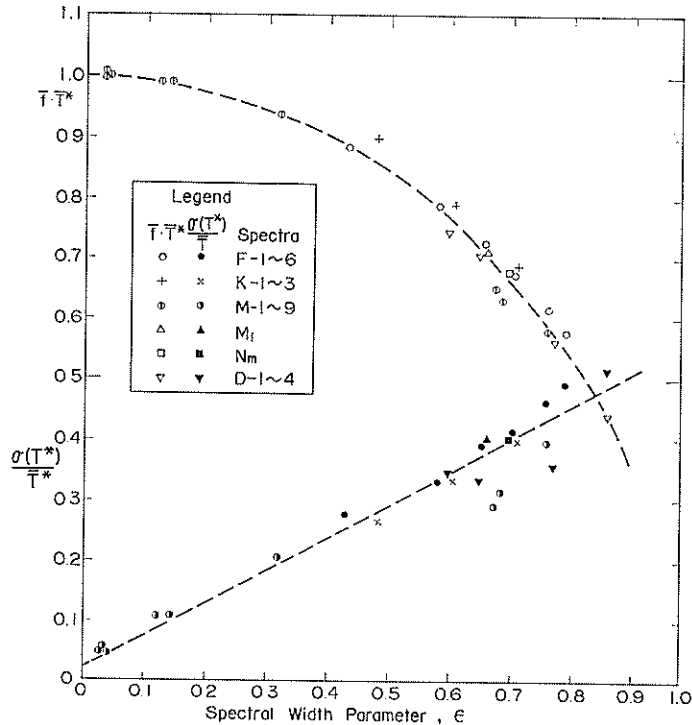


Fig. 17. Mean and standard deviation of non-dimensional crest-to-trough wave periods

wave period, \bar{T}^* , which is normalized by multiplication with the mean frequency \bar{f} , steadily decreases as ϵ increases. On the other hand, the ratio of standard deviation to mean wave period increases as ϵ increases though some scatter of data are observed.

5.2 Zero-up-Cross Wave Heights

Unlike the crest-to-trough wave heights, the zero-up-cross wave heights show the distribution quite close to the Rayleigh distribution. Figure 18 shows the comparison of the observed wave height distributions with the theoretical one of Eq. 13 for the model spectra of M-5, F-4, and D-4. For each wave spectrum, the observed frequencies of wave heights in five to ten runs were summed up for each range of wave heights and averaged to give the density of wave height appearance. Among these examples shown in Fig. 18, the wave spectrum D-4 which has conspicuous double peaks exhibits some deviation from the Rayleigh distribution.

Wave Statistics with Spectral Simulation

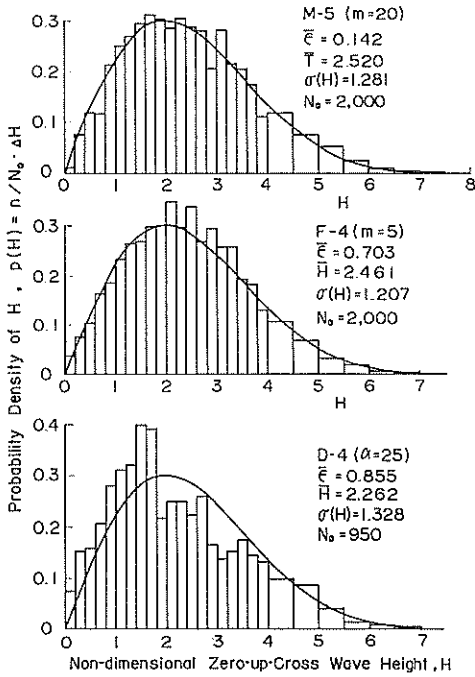


Fig. 18. Examples of the distribution of zero-up-cross wave heights

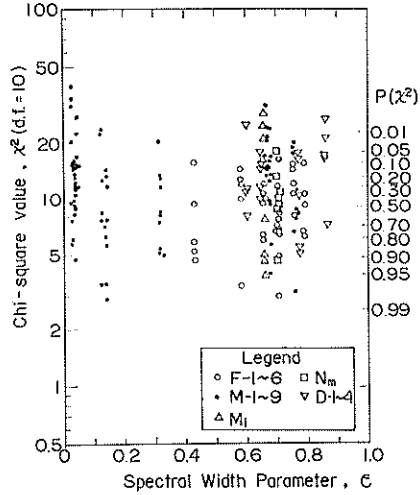


Fig. 19. Scatter diagram of the chi-square value of wave heights under the assumption of the Rayleigh distribution

The fitness of the Rayleigh distribution to the observed ones was examined by the chi-square test for each run. The range of wave height from 0 to ∞ was divided into ten subranges in such a way that each subrange has the probability of $\Delta P=1/10$. The chi-square values of all the runs except for the K-series spectra are shown in Fig. 19 against the spectral width parameter ϵ . The chi-square values are distributed in the range from 2.9 to 40.0, which corresponds to the probability of 0.98 to less than 0.01. The scatter of χ^2 seems to be little affected by the spectral width parameter ϵ . The result of Fig. 19 suggests that the Rayleigh distribution fits to the zero-up-cross wave height in general, regardless

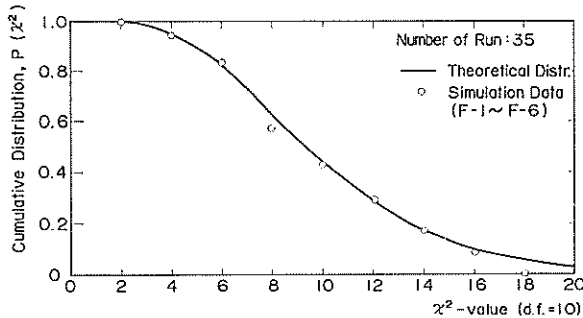


Fig. 20. Cumulative distribution of the chi-square value for the test of the fitness of the Rayleigh distribution to the wave height

of the width of wave spectra. Since the chi-square value itself exhibits a distribution in a certain range even if the population of the data exactly fits to the proposed distribution, the test by a single value of chi-square is not conclusive to examine the proposed distribution. Thus, the cumulative distribution of chi-square values of 35 runs for the wave spectra of F-1 to F-6 which correspond to Pierson-Moskowitz's spectrum is compared in Fig. 20 with the theoretical one of chi-square value. The agreement between the observed values and theoretical one suggests the fitness of the Rayleigh distribution to the population of zero-up-cross wave heights for wind waves.

Another examination of wave height distribution was made for the heights of various mean waves. Figure 21 shows the average values of $H_{1/3}$, \bar{H} , and $\sigma(H)$ for each spectrum against the spectral peakedness Q_p defined by Eq. 44 in 2.5. These average values steadily decrease from the theoretical values of Eqs. 15 and 20 as the spectral peakedness decreases. The use of ϵ as the abscissa has not yielded such steady decreases but produced scatter of data. The average ratios of H_{\max} , $H_{1/10}$, and \bar{H} to $H_{1/3}$ for each wave spectrum are shown in Fig. 22 against Q_p . Again, steady deviations from the theoretical values with the decrease of Q_p are observed.

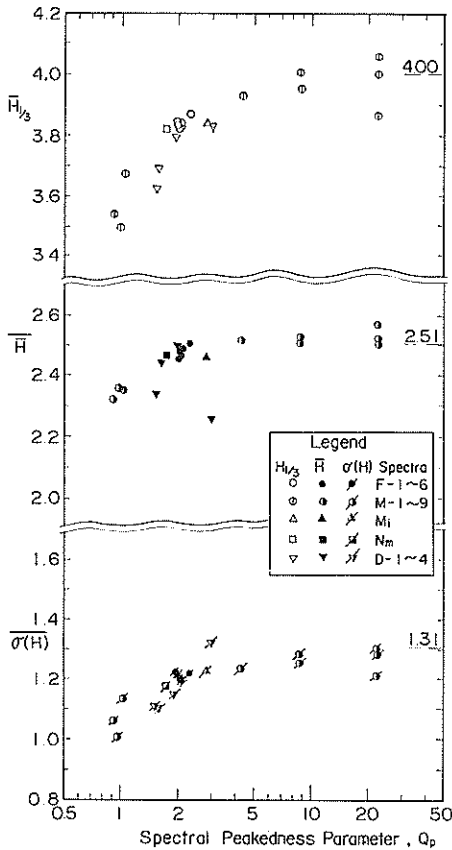


Fig. 21. Significant value, mean value, and standard deviation of zero-up-cross wave heights

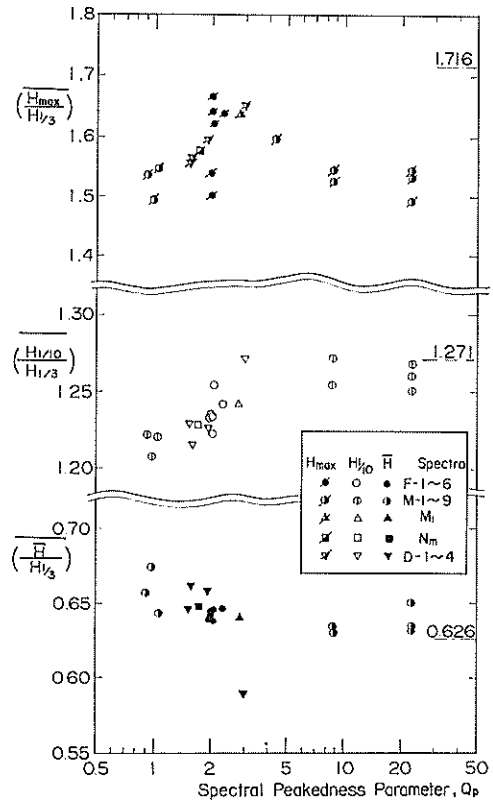


Fig. 22. Ratios of representative wave heights to significant wave height

In Figs. 21 and 22, all the data except for $(\overline{H_{\max}/H_{1/3}})$ approach the theoretical values as Q_p increases. This is expected because as shown in Fig. 2 a very large value of Q_p is associated with a very small value of ϵ , which guarantees the applicability of the Rayleigh distribution. The deviation of $(\overline{H_{\max}/H_{1/3}})$ from the theoretical value of 1.716 for 200 waves at large values of Q_p seems to be caused by the existence of a high level of auto-correlation in each wave height train with large Q_p , since the theory presumes the sample of N wave heights chosen at random from the population. The situation is the same with the distribution of $(\overline{\eta_{\max}})_{\max}$ shown in Fig. 13.

Like the highest maximum of surface elevation, the highest wave height in a sample of N waves varies from a sample to another. Figure 23 shows the distribution of the ratio of $H_{\max}/H_{1/3}$ observed in simulated wave trains. The model wave spectra of F-1 to F-6 with f^{-5} type, M-6 with f^{-10} type, M_2 of Mitsuyasu's one, and N_m of Neumann's one were employed to provide the data of 65 runs in total. The theoretical distribution was calculated from Eq. 40 by setting $H_{\max}=2\eta_{\max}$ and introducing the relation of $H_{1/3}=4.00\sigma$. Although the observed data of H_{\max} were obtained in the trains of 200 zero-up-cross waves, their distribution is closer to the theoretical one for the sample of 100 waves rather than to that for 200 waves. One possible cause of difference is the limitation in the number of component waves employed in wave simulation, and another is the use of 200 continuous waves instead of 200 random samples from the population.

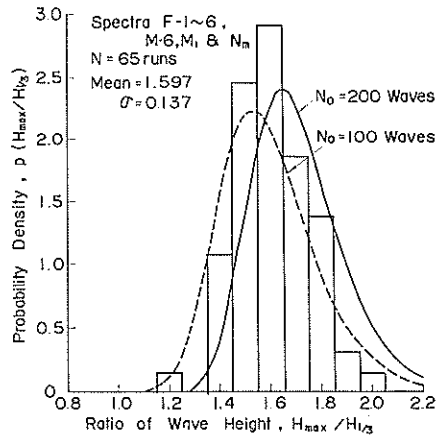


Fig. 23. Distribution of the maximum wave height in terms of significant wave height in a train of 200 waves

5.3 Zero-up-Cross Wave Periods

Distributions of zero-up-cross wave periods are shown in Fig. 24 for the model wave spectra of M-5, F-4, and D-4. Like Figs. 16, 18, etc., the ordinate shows the density of wave period at respective positions calculated as the average of five to ten runs for each wave spectrum. The theoretical distribution of Eq. 21 proposed by Bretschneider (1959) is in fair agreement with that of F-4 spectrum, but it is in disagreement with those of M-5 and D-4 spectra.

General characteristics of wave periods are shown in Figs. 25 and 26 against the spectral width parameter ϵ . Figure 25 shows the average values of significant and mean wave periods normalized by multiplication with the mean frequency defined by Eq. 63 in 3.3 for each wave spectrum. The normalized significant wave period tends to increase as ϵ increases from the value of 1.0 to 1.28, while the normalized mean wave period shows a tendency to decrease from 1.0 to 0.85 as ϵ increases. Since the increase of $\bar{f} \cdot T_{1/3}$ and decrease of $\bar{f} \cdot \bar{T}$ is not large, $T_{1/3}$ and \bar{T} may be regarded approximately equal to $1/\bar{f}$ in practice of field wave data analysis. The standard deviation of wave periods, being expressed as the ratio to the mean wave period, steadily increases from 0 to 0.5 with the increase of ϵ . The data of $T_{1/3}$, \bar{T} , and $\sigma(T)$ are fitted with the empirical curves drawn with dashed lines

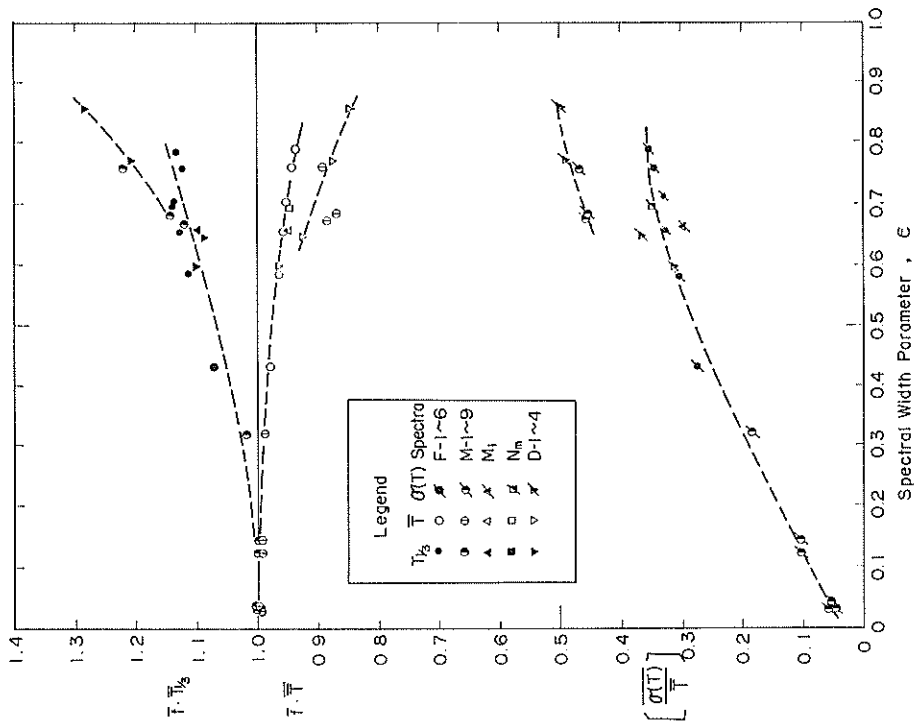


Fig. 25. Significant wave period, mean wave period, and standard deviation of wave period by zero-up-cross method

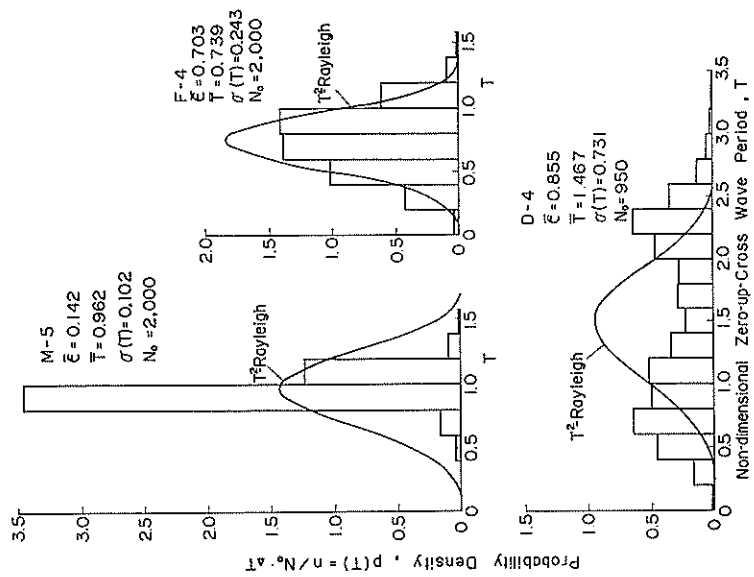


Fig. 24. Examples of the distribution of zero-up-cross wave periods

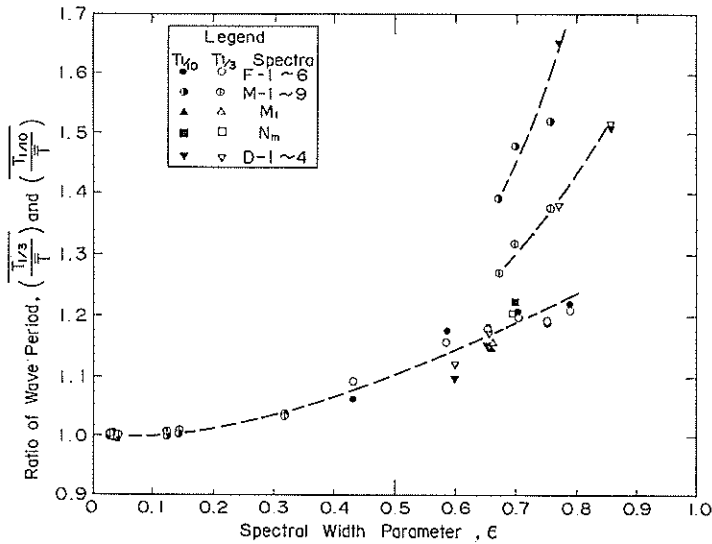


Fig. 26. Ratios of the periods of one-tenth maximum wave and significant wave to the period of mean wave

in Fig. 25. Though drawing of these curves is rather subjective, the wave spectra of M-7, 8, and 9 with flat spectral shapes and those of D-3 and D-4 with conspicuous double peaks constitute a group of data different from the rest of the model wave spectra. This separation of data suggests that some parameter other than the spectral width is playing a controlling role on the characteristics of zero-up-cross wave periods; the spectral peakedness, however, has been found unimportant. The significant wave period and that of one-tenth highest waves in terms of the ratios to the mean wave period are plotted in Fig. 26 against the spectral width parameter ϵ . Except for the data of the model wave spectra of M-7, M-8, M-9, D-3, and D-4, $T_{1/3}$ and $T_{1/10}$ are almost equal and they show a slight increase from 1.0 to 1.22 as ϵ increases from 0 to 0.79. The periods of maximum waves have also been found to have almost the same values with $T_{1/10}$ and $T_{1/3}$ except for the spectra of M-7, M-8, M-9, and D-3, which have the tendency of increase from $T_{1/3}$ through $T_{1/10}$ to T_{max} .

5.4 Correlation between Wave Heights and Periods

Figure 27 is an example of scatter diagram of wave height versus wave period. The wave spectrum is F-4 of f^{-3} type with the cut-off frequency of $f_{max}=5.0$. The data of 200 zero-up-cross waves in one simulated

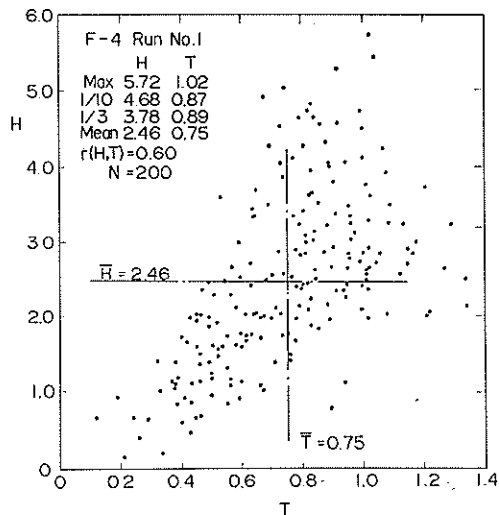


Fig. 27. Example of scatter diagram of zero-up-cross wave height versus period

wave train are shown in this diagram. It is seen that the portion of the data lower than the mean values of wave heights and periods show a close correlation but the higher portion does not show marked correlation. This uncorrelation between the heights and periods of large waves has yielded quasi-equality among $T_{1/3}$, $T_{1/10}$, and T_{\max} discussed in the previous section. The overall correlation between wave heights and periods is measured with the correlation coefficient defined by

$$r(H, T) = \frac{1}{\sigma(H) \cdot \sigma(T)} \cdot \frac{1}{N} \sum_{i=1}^N (H_i - \bar{H}) \cdot (T_i - \bar{T}). \quad (67)$$

The correlation coefficient of the data shown in Fig. 27 has been calculated as 0.60. For each run of a model wave spectrum the correlation coefficient has been calculated and the mean value of correlation coefficient has been obtained for each wave spectrum. Figure 28 is the result of the calculation, showing $\overline{r(H, T)}$ against ϵ . The correlation coefficient between zero-up-cross wave heights and periods is

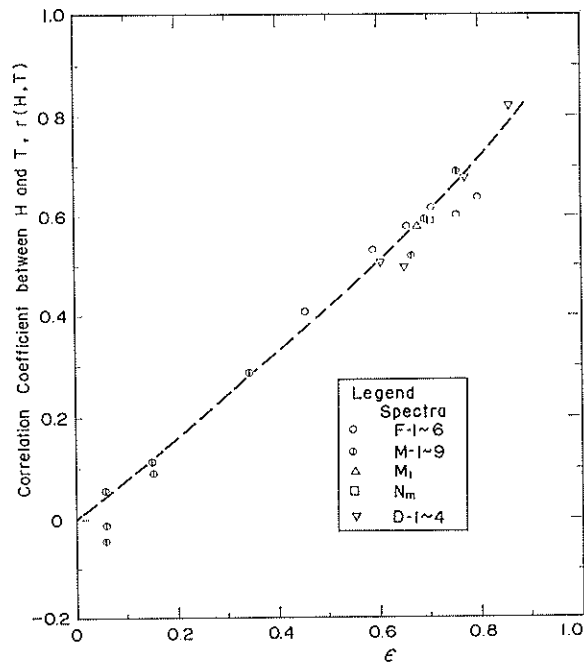


Fig. 28. Correlation coefficient between heights and periods of zero-up-cross waves

strongly controlled by the spectral width parameter. On the other hand, the correlation coefficient between crest-to-trough wave heights and periods shows some scatter when plotted against ϵ as seen in Fig. 29. In any case such clear relation between the correlation coefficient and the spectral width parameter has not been reported for actual wave records. Bretschneider (1959) has reported the values of correlation coefficient between wave heights and lengths from 0.08 to 0.65 for wind waves recorded by step-resistance wave staffs, but the respective value of spectral width parameter have not been given. Instead, he has given

Wave Statistics with Spectral Simulation

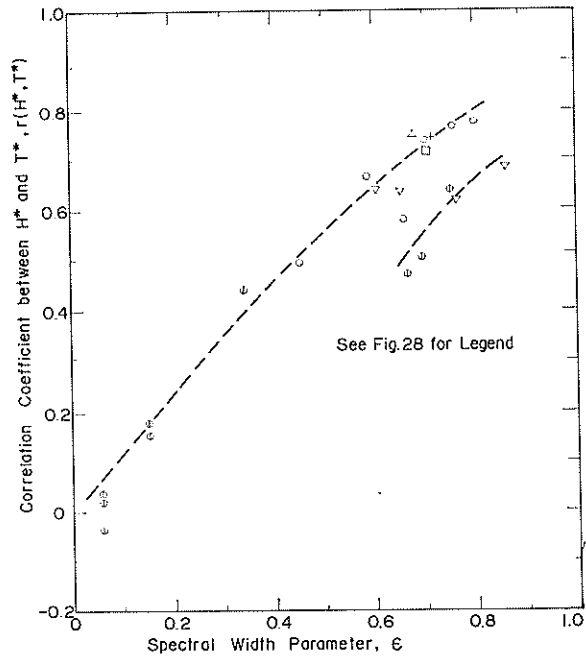


Fig. 29. Correlation coefficient between heights and periods of crest-to-trough waves

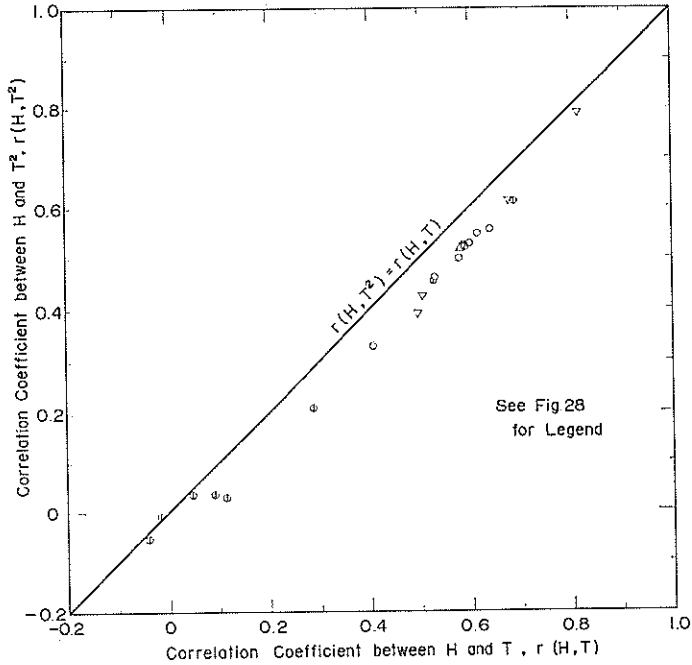


Fig. 30. Correlation coefficient between wave height and length versus correlation coefficient between wave height and period by zero-up-cross method

the relationship between $r(H, T^2)$ and ϵ as the deep water wave generation parameter. According to the relationship given, $r(H, T^2)$ is 1.0 at $\epsilon=0.464$ and decreases toward 0 as ϵ increases toward 1.0. The relationship is just opposite to the data shown in Figs. 27 and 28. Since Bretschneider's data exhibit large scatter and are not conclusive, the analysis of field data will be required to determine whether the relation of Figs. 27 and 28 is applicable to actual wave record.

Though the correlation coefficient employed by Bretschneider is that between wave heights and lengths (or square of wave period), it does not differ much from that between wave heights and periods. Figure 30 shows the relation between $r(H, T^2)$ and $r(H, T)$. The correlation coefficient $r(H, T^2)$ is slightly smaller (0.1 at most) than $r(H, T)$, but it is uniquely determined by the latter.

6. Length of the Run of Wave Heights

6.1 Theory of the Length of a Run

A run of wave heights is defined as the sequence of waves, the heights of which exceed a predetermined value: e.g., $H_{1/3}$, H_{median} , etc. In an example of the sequence of wave heights shown in Fig. 31, ten waves out of fifty one exceed $H_{1/3}$ in height; they constitute seven runs of $H > H_{1/3}$. The length of a run is

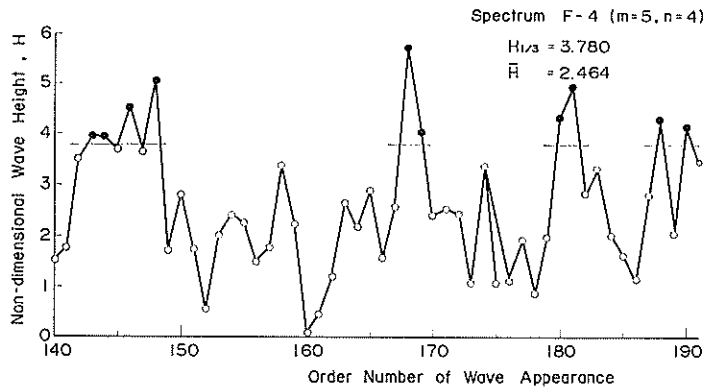


Fig. 31. Example of sequence of wave heights

the number of waves in that run. In the example of Fig. 31 the run length is one or two; the mean run length is 1.43. The concept of the run of wave heights has a practical importance in several design problems. The quantity of overtopping of a sea wall by irregular waves, for example, is affected by the number of large waves which attacks the sea wall in sequence. If large waves come at random, the ratio of overtopping may be estimated for a design purpose with the average over all waves. If large waves have tendency to come in a group, however, the average over large waves only may be recommended.

The length of a run is calculated with the probability that a phenomenon in question will occur at one trial. Let the probability be P , and the probability not occurring Q . Clearly there exists the relation

$$Q=1-P. \quad (68)$$

The run with the length j is defined such that the phenomenon occurs at $(j-1)$ consecutive trials after one occurrence of the phenomenon and fails to occur at the j -th trial. If the process is random and not affected by the result of preceding trial, the probability of the run with the length of j , denoted by $P_1(j)$, is expressed as

$$P_1(j) = P^{j-1}Q. \quad (69)$$

The mean length denoted by \bar{j}_1 is calculated with Eq. 69 as its first moment:

$$\bar{j}_1 = E(j_1) = \sum_{j=1}^{\infty} j P_1(j) = \frac{1}{Q}. \quad (70)$$

For the calculation of the standard deviation, the second moment of $P_1(j)$ is obtained as

$$E(j_1^2) = \sum_{j=1}^{\infty} j^2 P_1(j) = \frac{1}{Q^2}(1+P). \quad (71)$$

The standard deviation is therefore obtained as

$$\sigma(j_1) = \sqrt{E(j_1^2) - \bar{j}_1^2} = \frac{P}{Q}. \quad (72)$$

Next, a total run is defined as the run beginning at the first occurrence of a phenomenon, continuing the period of non-occurrence, and ending at the first re-occurrence of the phenomenon. A portion of wave height train from the exceedance beyond $H_{1/3}$ to the next exceedance is an example of a total run. The length of the total run from $H_{1/3}$ to $H_{1/3}$ is approximately the number of waves from a peak of wave height train to the next peak, or the recurrence interval of high waves. The probability of a total run with a length of j , denoted by $P_2(j)$, is given by

$$P_2(j) = \frac{PQ}{P-Q}(P^{j-1} - Q^{j-1}). \quad (73)$$

The mean and standard deviation of the length of a total run are calculated as

$$\bar{j}_2 = \frac{1}{P} + \frac{1}{Q} \quad (74)$$

$$\sigma(j_2) = \sqrt{\frac{P}{Q^2} + \frac{Q}{P^2}}. \quad (75)$$

The results of Eqs. 74 and 75 are expected since a total run is the sum of the runs of occurrence and non-occurrence.

6.2 Observed Lengths of the Runs of Wave Heights

All the simulated wave records were analysed for the runs of wave heights. Three definitions of runs were used: one with waves exceeding the median wave height H_{median} , the second one with waves exceeding the significant wave height $H_{1/3}$, and the last one with a total run from $H_{1/3}$ to $H_{1/3}$. The probability of a wave height exceeding the median value is simply $\frac{1}{2}$: hence $P=Q=\frac{1}{2}$. The pro-

bability that a wave exceeds the significant wave in height is 0.134 provided that the wave heights follow the Rayleigh distribution. Observed value of this probability, defined as the ratio of the number of waves exceeding the significant wave heights to the total number of waves in one simulated wave records, varied from 0.130 to 0.149 as the average for five to ten runs of each wave spectrum except for the K-series spectra. The overall average and standard deviation of the observed probability for 159 runs are

$$P(H > H_{1/3}) = 0.1386 \pm 0.0178 . \quad (76)$$

This average value is slightly larger than the theoretical value of 0.134 by the amount of 0.005. The difference is partly attributed to the limit in the number of zero-up-cross waves in a run, i.e., $N_0=200$. Slight deviation of the observed wave height distribution from the Rayleigh distribution such as indicated in Fig. 22 is another cause of the difference.

Distributions of the lengths of three wave runs defined in the above are shown in Fig. 32 for the model wave spectra of F-4, M-5, and M-9. For comparison

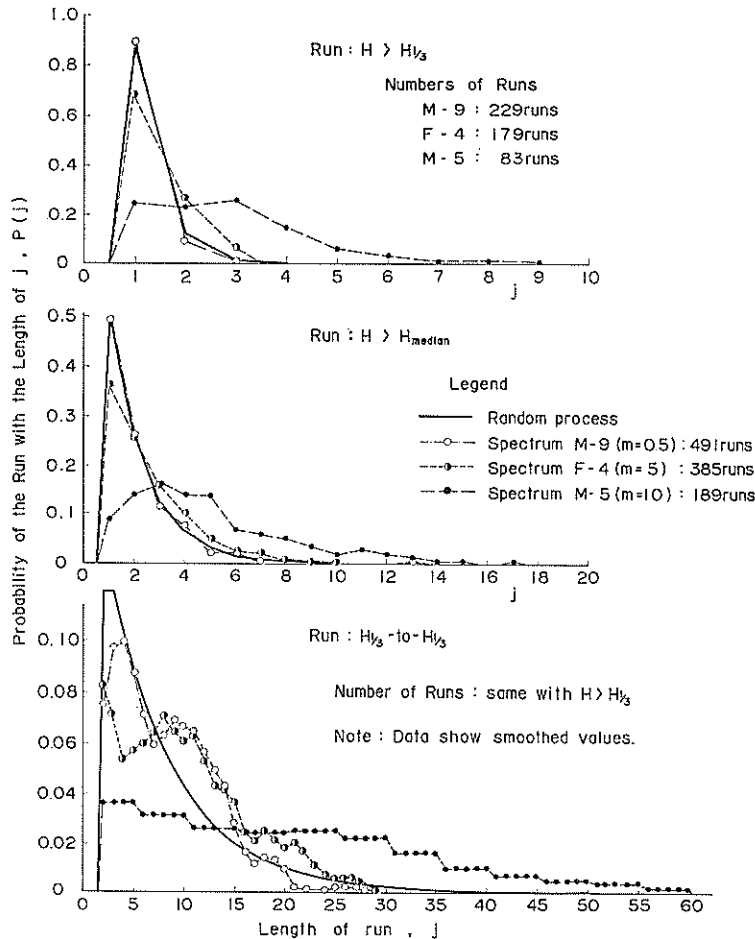


Fig. 32. Examples of the distribution of the length of runs of wave heights

Wave Statistics with Spectral Simulation

the distributions of the run lengths in a random process have been calculated by Eqs. 69 and 73 with $P=Q=\frac{1}{2}$ for $H>H_{\text{median}}$ and with $P=0.1386$ and $Q=0.8614$ for $H>H_{1/3}$ and $H_{1/3}$ -to- $H_{1/3}$ runs. The spectrum M-9 of $f^{-0.5}$ type which has almost uniform power density from $f_{\text{min}}=0$ to $f_{\text{max}}=5.0$ exhibits the run lengths almost same with those of random process. This is expected because a random process is represented with a white spectrum. On the other hand, the spectrum M-5 of f^{-10} type which has a marked peak at $f_0=1.0$ shows broad distributions of the lengths of the runs of wave heights. For example, a run of wave heights greater than the significant wave height may last for 9 waves, and a total run of wave heights from $H_{1/3}$ to $H_{1/3}$ may last for 60 waves. This means that large waves tend to come in a series, associated with a long series of small waves. The spectrum F-4 which represents a spectrum of wind waves shows a little broader distributions of the run length than those of random process, but the difference is small. Hence, the length of a run of heights of wind waves may be

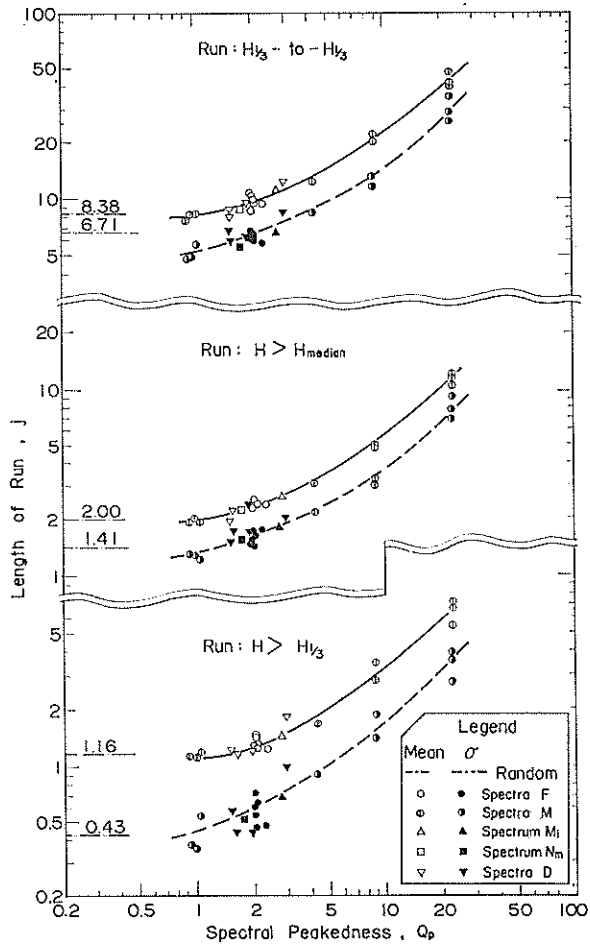


Fig. 33. Mean and standard deviation of the lengths of the runs of wave heights

approximated with that of the random process.

The effect of spectral peakedness on the length of a run of wave heights is shown in Fig. 33, where means and standard deviations of the lengths of the three runs of wave heights are plotted against the spectral peakedness parameter Q_p . The mean and standard deviation calculated as a random process provides the asymptotic values for the run of $H > H_{1/3}$, but they give a little larger values than actual asymptotic values of observed data for the runs of $H > H_{\text{median}}$ and $H_{1/3}$ -to- $H_{1/3}$. As the spectral peakedness increases, the means and standard deviations of the run lengths steadily increase from these asymptotic values. A plotting with the spectral width parameter as the abscissa has failed to produce such a clear relationship. Thus the controlling factor appears to be the spectral peakedness, not the spectral width.

It is interesting to note that the mean length of the total run for $H_{1/3}$ -to- $H_{1/3}$ is about nine for the model spectra corresponding to that of wind waves. This means that a peak of wave height greater than the significant wave comes in the period of about nine waves on the average. It should be mentioned however that the run length is determined statistically only. Take the run of heights exceeding the median wave height. The mean length in a random process is 2.0. But, 50% of runs have the length of 1.0 (only one wave exceeds the median and the next wave goes under), while 6.25% of runs have the length not less than 5.0. The variability in the run length is reflected in large values of the standard deviation in comparison with the mean as seen in Fig. 33. Application of the concept of a run of wave heights for practical problems will require attention to the variability in the run length as well as to the mean length.

7. Discussion of the Results of Wave Simulation for Practical Application

7.1 Number of Component Waves for Laboratory Reproduction of Ocean Waves

Recently many efforts have been poured upon the laboratory reproduction of ocean waves. One of the successful methods is the use of automatically controlled wave paddle, the movement of which follows a predetermined oscillation of irregular nature. The oscillation is calculated by a digital computer for a given wave spectrum and fed into the system through a magnetic or perforated paper tape. The calculation of irregular oscillation for the preparation of input tape can be done in the way similar with the present wave simulation; a difference is the addition of a transform function for wave generation characteristics. A factor to be determined is the sufficient number of component waves to be able to reproduce the ocean waves. In a simpler system, the input oscillation is electrically produced by the mixing of electric currents from several oscillators. Here again the number of oscillators becomes a point of argument. The answer can be obtained from the result of the present wave simulation.

The model wave spectra of K-1, K-2, and K-3 have been given the component waves of only three, five, and ten, respectively. The limit in the number of component waves were intentionally made to simulate an irregular wave generator of simple system. According to the result of the simulation, a limit in the number of component waves restricts the occurrence of large η_{max} and lowers the kurtosis of surface elevation. Figure 34 shows the variation of the highest maximum,

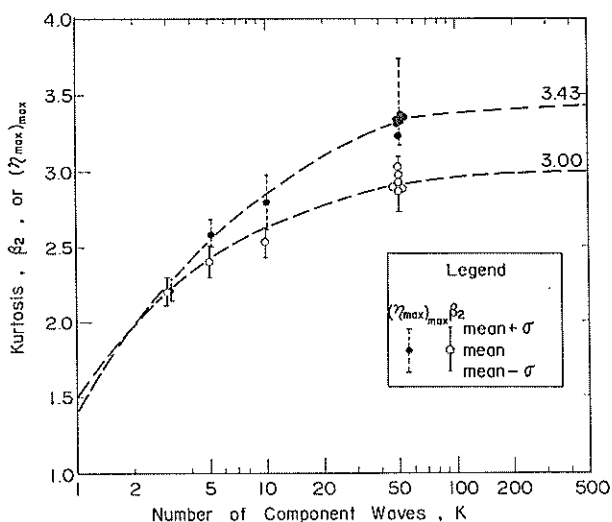


Fig. 34. Effect of wave component numbers on the distribution of surface elevation

$(\eta_{\max})_{\max}$, in a train of zero-up-cross waves and that of the kurtosis against the number of component waves. The data of wave spectra F-1 to F-6 are also shown to represent the case of fifty component waves. The limiting case of $K=1$ is a regular sinusoidal wave, for which $(\eta_{\max})_{\max} = \sqrt{2} \sigma$ and $\beta_2 = 1.5$. The results of simulation is shown with the mean value and the range of one standard deviation. Figure 34 clearly shows that the component waves of ten or less are insufficient to reproduce the Gaussian process of surface elevation. Even the component waves of fifty employed in the present simulation appear to be not large enough. The trend of data suggests that more than two hundred component waves are necessary to reproduce that the Gaussian process of surface elevation.

The effect of the number of component waves on the distribution of wave heights is demonstrated in Fig. 35, which shows the variations of H_{\max} , $H_{1/10}$, and \bar{H} in terms of $H_{1/3}$ versus the component number, K . The trend of the data is the same with Fig. 34, suggesting more than two hundred component waves necessary for the complete reproduction of a wave train with the Rayleigh distribution for wave heights. It should be noted however that the results of wave simulation with fifty component waves do not differ much from those of the Gaussian distribution of surface elevation and of the Rayleigh distribution of wave heights. This little difference has been one of the reasons to choose the number of fifty for that of component waves as a compromise between the computation time and the realization of the theoretical distributions.

For the laboratory simulation of ocean waves, the results of Figs. 34 and 35 indicates that the number of ten for component waves is apparently insufficient; the number of two hundred will be sufficient if it is feasible. The discussion, however, is based on the presumptions of the Gaussian distribution for surface elevation and the Rayleigh distribution for wave heights. Actual waves exhibit non-linearity in surface elevation and some deviation in wave height distribution. Such behaviors of actual waves suggest the number of component waves necessary for the laboratory simulation somewhat smaller than two hundred; the

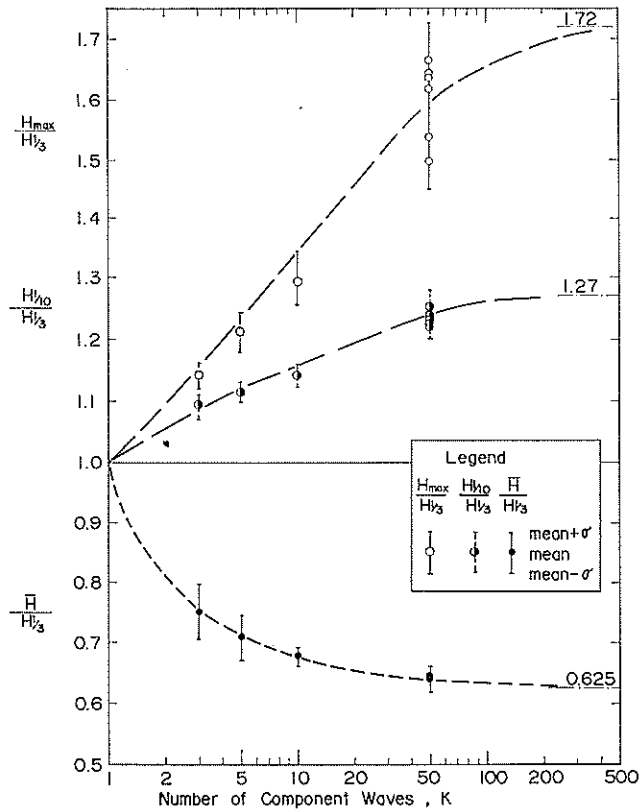


Fig. 35. Effect of wave component numbers on the distribution of wave heights

number of fifty to one hundred will be practical for the preparation of input tapes and that of thirty for electric oscillators.

7.2 Wave Heights and Periods of a Double Peaked Spectrum

A double peaked spectrum is observed when wind waves are generated on the water surface where a swell from a remote source of disturbance is present. On such occasions, engineers are often asked to estimate the representative height and period of the superimposed wave system from the independent data of wind waves and swells. Engineer's practice is the use of the following equations based on the summation of wave energy.

$$H_{total} = \sqrt{H_1^2 + H_2^2}, \tag{77}$$

$$T_{total} = \sqrt{\frac{H_1^2 + H_2^2}{\frac{H_1^2}{T_1^2} + \frac{H_2^2}{T_2^2}}}, \tag{78}$$

where H and T are the height and period of the significant wave or some other representative wave, respectively.

The first equation is implicitly verified in Fig. 23. The fact that the wave

heights of the model wave spectra of D-series with double peaks follow the Rayleigh distribution is the proof. As explained in 3.3, the simulated surface elevation has been normalized with its root-mean-square value, σ . The square of σ , or the variance, is equal to two times the integral of power spectral density regardless of spectral shape (Eq. 9). Since a double peaked spectrum is considered to be formed by the superposition of two wave trains, each with a single peak in the spectrum, the variance of superposed wave system is the sum of the variances of two wave trains. This holds as a general rule within the limit of linear wave spectral theory. If the two wave trains and the superposed wave system have the same distribution function for the wave heights, then the relation of Eq. 77 does hold; otherwise not. In the present case, a single peaked wave spectrum regardless of its shape has been shown to approximately produce the Rayleigh distribution for wave heights and so does a double peaked wave spectrum. This supports the applicability of Eq. 77 to the system of swells and wind waves.

The above consideration yields the possibility to estimate the height of swell component H_1 from the data of the wave height and power spectrum of an observed wave record. The formula is

$$H_1 = H_{total} \times \sqrt{\frac{E_1}{E}}, \quad (79)$$

where:

$$\left. \begin{aligned} E_1 &= 2 \int_0^{f_1} S(f) df, \\ E &= 2 \int_0^{\infty} S(f) df, \end{aligned} \right\} \quad (80)$$

in which f_1 is the frequency at which the power spectrum shows a hump.

The applicability of Eq. 78 is examined in Table 3, which lists the estimated values of wave periods by Eq. 78 and the observed values in the simulation. In the estimation, the height of low frequency waves H_1 was calculated by Eq. 79 with the ratio of wave energy which was obtained from the power spectrum as listed in Table 3. The height of high frequency waves was calculated from Eq. 79. The periods of low and high frequency waves were estimated from the result of single peaked spectra. The result of the estimation of wave period shows a fair agreement for the significant wave period, but the agreement for the mean wave period is excellent. The discrepancy of the estimated values of significant

Table 3. Comparison of Estimated and Observed Wave Periods of Double Peaked Wave Spectra

Spectra	f_1	E_1/E	Mean Wave Period		Significant Wave Period	
			(1)*	(2)**	(1)*	(2)**
D-1	0.60	0.035	0.782	0.788	0.909	0.899
D-2	0.63	0.152	0.828	0.822	0.951	0.966
D-3	0.66	0.473	1.013	1.018	1.152	1.407
D-4	0.72	0.818	1.472	1.467	1.619	2.217

* Estimated values by Eq. 79.

** Average of the observed values in wave simulation for each spectrum.

periods from the observed values for the model wave spectra D-3 and D-4 has been suggested in Fig. 26, where the ratio of $T_{1/3}/\bar{T}$ for the spectra D-3 and D-4 was excessively large in comparison with other data. It is not clear whether this is a singular phenomenon in the wave simulation. The difference between the mean wave period and the significant wave period, however, is small in the field wave records. Thus the agreement for the mean wave period is considered to support the applicability of Eq. 78 to the problem of the superposition of irregular waves in the field.

7.3 Applicability of the Rayleigh Distribution for Wave Heights

A feature of the results of present wave simulation is the fitness of the Rayleigh distribution for zero-up-cross wave heights as demonstrated by the chi-square test shown in Figs. 19 and 20. The ratios among several representative wave heights, such as $H_{1/10}$, $H_{1/3}$, etc., on the other hand, are generally lower than the theoretical values estimated by the Rayleigh distribution. The results of the chi-square tests and the examination of wave height ratios is contrary to the actual ocean wave data. Goodknight and Russel (1963) have reported that surface wave heights during hurricanes recorded with a step-resistance wave staff did not follow the Rayleigh distribution exactly according to the chi-square test, but the wave height ratios were practically in agreement with the theoretical values. Goda and Nagai (1968) have also observed similar tendency for wind waves recorded with a capacitance probe at Nagoya Port; the maximum wave height was in general greater than the statistically expected value.

The difference between the wave statistics in the present wave simulation and the field observation is attributed to the non-linearity of surface elevation which is defected in the wave simulation. Wave records at Nagoya Port have clearly exhibited positive skewness and large kurtosis. The non-linearity works to increase the height of higher maxima in surface elevation, thus increasing the heights of large waves. The ratio of mean wave height to the root-mean-square value of η will be decreased by the presence of non-linearity; an addition of second harmonic to a sinusoidal wave profile increases σ , but the wave height remains unchanged. A few trials to introduce the non-linearity in surface elevation into the process of spectral wave simulation have been unsuccessful. Hence, the effect of non-linearity on wave statistics suggested in the above has not been verified but remains as a speculation.

Another source of the difference between the present wave simulation and the field data is the use of a finite number of component waves to simulated wave profiles. As discussed in 7.1, a decrease in the number of component waves works to lower the heights of large waves especially of maximum waves. Use of fifty to sixty component waves in the present wave simulation instead of a greater number of waves seems to have interfered the realization of statistically expected heights of maximum waves to some extent.

The difference between the simulated wave heights and the theoretical values based on the Rayleigh distribution is not large, however. As seen in Figs. 21 and 22 the difference is less than 10% for most of the model wave spectra inclusive of double peaked spectra. With the addition of non-linearity and the increase in the number of component waves, the wave heights are expected to approach the theoretical values. Thus, the Rayleigh distribution is considered applicable for the heights of waves defined by the zero-up-cross method, regardless of the func-

tional shape of power spectrum.

It is interesting to note that a wave record obtained in a shallow water tends to show the distribution of wave heights narrower than the Rayleigh distribution, especially as the significant wave height increases in comparison with the water depth (Goda 1967). This is easily understood as the result of selective breaking of large waves in a wave train at a shallow water. Wave spectra in the shallow water have been measured by Iwagaki and Kakinuma (1967) and by Ijima and Matsuo (1968). The spectra are known to have a smaller rate of density decrease at high frequency component such as expressed by f^{-3} instead of f^{-5} in the deep water. The change in the exponent of the frequency term of the power spectrum has been discussed by Hamada (1964) as a result of wave breaking in the shallow water. The model wave spectrum M-7 which has the exponent of -2.5 , however, has not shown a significant deviation of the distribution of wave heights from the Rayleigh distribution as demonstrated in Figs. 21 and 22. Therefore, the deviation of wave height distribution from the Rayleigh type at the shallow water should be considered separately from the change in the functional shape of wave spectrum. It must be a highly non-linear phenomenon, which needs full analysis with the theory of non-linear wave spectra.

8. Conclusions

Major conclusions of the present numerical experiments on wave statistics are summarized as follows;

(1) The distribution of the maxima of surface elevation is accurately described with the theory of Cartwright and Longuet-Higgins.

(2) The estimate of the spectral width parameter based on the numbers of maxima and zero-up-crossings agrees with that based on the moments of power spectrum, when the sampling of surface elevation is carried out with the time interval of $\Delta t \leq 1/(5f_{\max})$ in which f_{\max} denotes the cut-off frequency.

(3) The highest maximum of surface elevation in a continuous record of waves with a sharp spectral peak is a little lower than the statistically expected value, possibly because of the existence of a high level of auto-correlation.

(4) The distribution of wave heights defined by the *crest-to-trough* method becomes broader than the Rayleigh distribution as the spectral width parameter increases.

(5) The distribution of wave heights defined by the *zero-up-cross* method practically follows the Rayleigh distribution for the range of spectral width parameter from 0.03 to 0.86 irrespective of the spectral shape and cut-off frequency.

(6) A Rayleigh-type distribution for the square of wave period proposed by Bretschneider fairly agrees with that of wind waves, but it disagrees with that of the waves with a sharply peaked spectrum, double peaked spectrum, or flat spectrum.

(7) The mean wave period normalized with the mean spectral frequency slightly decreases with the increase of spectral width parameter, while the significant wave period slightly increases.

(8) The correlation coefficient between wave heights and periods defined by either the *crest-to-trough* method or the *zero-up-cross* method almost linearly increases with the increase of spectral width parameter.

(9) The length of the run of zero-up-cross wave heights increases as the peakedness of a power spectrum increases; for wind waves the run length does not differ much from that of random process.

(10) A decrease in the number of component waves for the simulation of irregular waves causes to make the distribution of surface elevations narrower than the Gaussian as well as that of wave heights narrower than the Rayleigh; for laboratory simulation of ocean waves more than fifty component waves are recommended.

(11) Use of energy concept to estimate the representative height and period of wave system composed of wind waves and swells is justified on the basis of the wave simulation data of double peaked spectra.

The numerical experiments reported herein have been conducted with the aid of a digital computer TOSBAC 3400 at the Computation Center of the Port and Harbour Research Institute.

References

- 1) BORGMAN, L. E. (1969): Ocean wave simulation for engineering design, *Jour. Waterways and Harbors Div., Proc. ASCE, Vol. 95, No. WW4*, pp. 557~583.
- 2) BRETSCHNEIDER, C. L. (1959): Wave variability and wave spectra for wind-generated gravity waves, *U.S. Army Corps of Engineers, Beach Erosion Board, Tech. Memo. No. 113*, 192 pp.
- 3) BRETSCHNEIDER, C. L. (1963): A one-dimensional gravity wave spectra, *Ocean Wave Spectra*, Prentice-Hall, Inc., pp. 41~56.
- 4) CARTWRIGHT, D. E. (1963): Discussion to Bretschneider's presentation at a Conference on *Ocean Wave Spectra, Proceedings*, Prentice-Hall, Inc., p. 57.
- 5) CARTWRIGHT, D. E. and LONGUET-HIGGINS, M. S. (1956): The statistical distribution of the maxima of a random function, *Proc. Royal Soc., A., Vol. 237*, pp. 212~232.
- 6) COLLINS, J. I. (1967): Wave statistics from Hurricane Dora, *Jour. Waterways and Harbors Div., Proc. ASCE, Vol. 93, No. WW2*, pp. 59~77.
- 7) DAVENPORT, A. G. (1964): Note on the distribution of the largest value of a random function with application to gust loading, *Proc. Inst. Civil Eng., Vol. 28*, June, pp. 187~224.
- 8) EWING, J. A. (1969): A note on wavelength and period in confused seas, *Jour. Geophysical Res., Vol. 74, No. 6*, pp. 1406~1408.
- 9) GODA, Y. (1967): Note on the presentation and utilization of wave observation data (*in Japanese*), *Tech. Note of Port and Harbour Res. Inst., No. 39*, pp. 237~255.
- 10) GODA, Y. and NAGAI, K. (1968): Wave observation at the Port of Nagoya, Second Report, —analysis of the records of wind-generated surface waves observed at the inside of the port— (*in Japanese*), *Tech. Note of Port and Harbour Res. Inst., No. 61*, 64 pp.
- 11) GOODKNIGHT, R. C. and RUSSEL, T. L. (1963): Investigation of the statistics of wave heights, *Jour. Waterways and Harbors Div., Proc. ASCE, Vol. 89, No. WW2*, pp. 29~55.
- 12) HAMADA, T. (1964): On the f^{-5} law of wind-generated waves, *Report of Port and Harbour Res. Inst., No. 6*, 16 pp.
- 13) HAMADA, T. (1965): The secondary interaction of surface waves, *Report of Port and Harbour Res. Inst., No. 10*, 28 pp.
- 14) HASSELMANN, K. (1962): On the non-linear energy transfer in a gravity-wave spectrum, Part I General theory, *Jour. Fluid Mech., Vol. 12, Pt. 4*, pp. 481~500.
- 15) HINO, M. (1967): A predictor filter and transformation filter for ocean waves (1) (*in Japanese*), *Proc. 14th Conf. Coastal Engineering in Japan*, pp. 21~28.
- 16) IJIMA, T. and MATSUO, T. (1968): Observation of surf waves by stereo-wave meter, *Coastal Engineering in Japan, Vol. 11*, pp. 43~52.

Wave Statistics with Spectral Simulation

- 17) ITO, Y., FUJISHIMA, M. and KITATANI, T. (1966): On the stability of breakwaters (*in Japanese*), *Report of Port and Harbour Res. Inst.*, Vol. 5, No. 14, 134 pp.
- 18) IWAGAKI, Y. and KAKINUMA, T. (1967): On the bottom friction factors off five Japanese coasts, *Coastal Engineering in Japan*, Vol. 10, pp. 13~22.
- 19) KINSMAN, B. (1965): *Wind Waves*, Prentice-Hall, Inc., p. 345.
- 20) LONGUET-HIGGINS, M. S. (1952): On the statistical distribution of the heights of sea waves, *Jour. Marine Res.*, Vol. XI, No. 3, pp. 245~265.
- 21) MITSUYASU, H. (1968): On the growth of the spectrum of wind-generated waves (1), *Report of Res. Inst. Applied Mech., Kyushu Univ.*, Vol. XVI, No. 55, pp. 459~482.
- 22) NEUMANN, G. (1953): On ocean wave spectra and a new method of forecasting wind-generated sea, *U.S. Army Corps of Engineers, Beach Erosion Board, Tech. Memo. No. 43*, 42 pp.
- 23) PIERSON, W. J. and MOSKOWITZ (1964): A proposed spectral form for fully developed wind seas based on the similarity theory of S. A. Kitaigorodskii, *Jour. Geophysical Res.*, Vol 69, No. 24, pp. 5181~5190.
- 24) RICE, S. O. (1944): Mathematical analysis of random noise, reprinted in *Selected Papers on Noise and Stochastic Processes*, Dover Pub., Inc., 1954, pp. 133~294.
- 25) SUZUKI, Y. (1969): Determination of approximate directional spectra for coastal waves, *Report of Port and Harbour Res. Inst.*, Vol. 8, No. 3, pp. 43~101.
- 26) TICK, L. J. (1963): Nonlinear probability model of ocean waves, *Ocean Wave Spectra*, Prentice-Hall, Inc., pp. 41~56.
- 27) TUCKER, M. J. (1963): Analysis of records of sea waves, *Proc. Inst. Civil Eng.*, Vol. 26, No. 10, pp. 305~316.
- 28) TSURUTA, S. and GODA, Y. (1968): Expected discharge of irregular wave overtopping, *Proc. 11th Conf. Coastal Engineering, London*, pp. 833~852.

Appendix A: List of Symbols

- a : amplitude of wavelet constituting ocean waves
 A : amplitude of component wave for simulation study
 C_K : factor employed to divide the frequency range (Eq. 47)
 E : the E -value in the P-N-J method
 $E(f)$: energy spectrum of ocean waves
 $E(j)$: moment of the length of a run
 f : frequency
 \bar{f} : mean frequency defined by Eq. 63
 f_0 : frequency at which a power spectrum shows the maximum density
 H : wave height defined by the zero-up-cross method
 H^* : wave height defined by the crest-to-trough method
 j : length of the run of wave heights
 K : number of component waves for simulation study
 L : duration of a wave record
 m_n : n -th moment of a power spectrum (Eq. 26)
 m, n : exponents of frequency in the power spectral function of Eq. 56
 m', n' : exponents of frequency in the double-peaked spectral function of Eq. 61
 N : numbers in general
 N_0 : number of zero-up-crossings in the record with a duration of L (cf. Eq. 30)
 N_1 : number of maxima in the record with a duration of L (cf. Eq. 30)
 $p(\)$: probability density of the variable inside the parentheses
 $p^*(x_{\max})$: probability density for the distribution of the highest in the sample of N maxima (Eq. 40)
 P : probability of occurrence
 $q(x)$: cumulative distribution of the maxima of surface elevation (Eq. 33)
 Q : probability of non-occurrence
 Q_n : spectral peakedness parameter defined by Eq. 44
 $r(H, T)$: correlation coefficient between wave height and period
 $S(f)$: two-sided power spectrum of surface elevation of ocean waves
 t : time
 T : wave period defined by the zero-up-cross method
 T^* : wave period defined by the crest-to-trough method
 x : non-dimensional quantity of η_{\max}/σ
 $\bar{\ }$: upper bar referring to arithmetic mean except for \bar{f}
 α : factor for relative magnitudes of two peaks of the spectrum of Eq. 61
 β : factor for relative positions of two peaks of the spectrum of Eq. 61
 $\sqrt{\beta_1}$: skewness of surface elevation defined by Eq. 3
 β_2 : kurtosis of surface elevation defined by Eq. 4
 γ : Euler's constant, 0.5772...
 ϵ : spectral width parameter defined by either Eq. 25 (ϵ_{spec}) or Eq. 31 (ϵ_{nos})
 Δf : width of frequency band
 Δt : time interval of wave simulation and data sampling
 η : surface elevation from the mean elevation
 μ_k : k -th moment of surface elevation

Wave Statistics with Spectral Simulation

- ξ : non-dimensional quantity of $Nq(x_{\max})$
- π : constant, 3.14159...
- σ : square root of the variance of surface elevation (Eq. 9)
- $\sigma(\)$: standard deviation of the variable inside the parentheses from its mean
- ϕ : phase of component wave
- Φ : Tucker's 'peakiness' (Eq. 43)
- χ^2 : chi-square value for the test of the goodness of the fitness of theoretical distribution

Appendix B. Table of the Summary

Identification	F-1	F-2	F-3	F-4
Input Data				
m	5.0	5.0	5.0	5.0
n	4.0	4.0	4.0	4.0
$f_{\min} \sim f_{\max}$	0.5~2.0	0.5~3.0	0.5~4.0	0.5~5.0
K	50	50	50	50
nos. of run	5	5	5	10
Distribution of η				
skewness	0.011(0.035) ²⁾	-0.003(0.057)	-0.019(0.076)	0.011(0.043)
kurtosis	2.939(0.145)	3.023(0.083)	2.875(0.093)	2.981(0.104)
max. η_{\max}	3.453(0.119)	3.305(0.164)	3.182(0.187)	3.432(0.355)
min. η_{\min}	-3.217(0.116)	-3.362(0.049)	-3.306(0.304)	-3.271(0.207)
Nos. of Waves				
ratio of N_0	0.998(0.029)	0.994(0.013)	0.991(0.014)	0.992(0.010)
ratio of N_1	0.987(0.023)	0.992(0.014)	0.982(0.011)	0.990(0.020)
(e)nos.	0.430(0.037)	0.584(0.028)	0.653(0.009)	0.703(0.015)
(e)spec.	0.452(0.000)	0.588(0.000)	0.660(0.000)	0.705(0.000)
Crest-to-Trough				
η_{\max}	1.147(0.025)	1.029(0.020)	0.963(0.009)	0.899(0.032)
$\sigma(\eta_{\max})$	0.728	0.787	0.805	0.850
\bar{H}^*	2.289(0.051)	2.057(0.039)	1.921(0.023)	1.806(0.050)
$\sigma(H^*)$	1.296	1.344	1.370	1.371
T^*	0.748(0.015)	0.624(0.009)	0.568(0.006)	0.525(0.012)
$\sigma(T^*)$	0.202	0.207	0.222	0.218
$r(H^*, T^*)$	0.492(0.055)	0.663(0.028)	0.581(0.032)	0.740(0.013)
$H^* - \chi_{20}^2$: median ¹⁾	28.7	63.3	148.5	217.3
Zero-up-Cross				
$H_{1/3}$	3.868(0.043)	3.839(0.028)	3.837(0.050)	3.837(0.037)
\bar{H}	2.500(0.048)	2.476(0.018)	2.470(0.022)	2.461(0.032)
$\sigma(H)$	1.216	1.209	1.206	1.207
$H_{\max}/H_{1/3}$	1.637(0.085)	1.621(0.131)	1.500(0.050)	1.540(0.081)
$H_{1/10}/H_{1/3}$	1.241(0.016)	1.253(0.031)	1.234(0.013)	1.235(0.026)
$\bar{H}/H_{1/3}$	0.647(0.017)	0.645(0.008)	0.644(0.008)	0.642(0.010)
$T_{1/3}$	0.901(0.008)	0.887(0.009)	0.882(0.014)	0.883(0.013)
\bar{T}	0.827(0.024)	0.768(0.010)	0.750(0.010)	0.739(0.007)
$\sigma(T)$	0.225	0.233	0.245	0.243
T_{\max}/\bar{T}	1.024(0.132)	1.141(0.055)	1.131(0.083)	1.230(0.087)
$T_{1/10}/\bar{T}$	1.061(0.029)	1.175(0.021)	1.174(0.039)	1.208(0.032)
$T_{1/3}/\bar{T}$	1.090(0.034)	1.155(0.014)	1.177(0.022)	1.196(0.019)
$r(H, T)$	0.408(0.078)	0.531(0.029)	0.581(0.032)	0.615(0.032)
$H - \chi_{10}^2$: median	5.9	12.6	9.5	7.2
Length of Run				
H_{median}	2.38±1.76 ³⁾	2.40±1.60	2.27±1.44	2.49±1.74
$H_{1/3}$	1.24±0.48	1.37±0.63	1.24±0.47	1.39±0.60
$H_{1/3}$ -to- $H_{1/3}$	9.37±5.91	9.70±6.37	9.47±5.99	10.02±6.12
$P(H > H_{1/3})$	0.135(0.010)	0.139(0.018)	0.136(0.006)	0.137(0.012)

Notes: 1) The median value of chi-square for the test of the goodness of the fitness of the Rayleigh distribution to wave heights.

2) The numerals inside parentheses are the standard deviations of the values representing one run.

of Statistics of Simulated Waves

F-5	F-6	K-1	K-2	K-3
5.0 4.0 0.5~7.0 50 5	5.0 4.0 0.5~10.0 50 5	5.0 4.0 0.7~2.0 3 9	5.0 4.0 0.6~3.0 5 9	5.0 4.0 0.5~5.0 10 10
-0.037(0.055) 2.878(0.142) 3.289(0.409) -3.433(0.395)	0.019(0.028) 2.904(0.185) 3.425(0.263) -3.268(0.261)	-0.003(0.004) 2.202(0.091) 2.214(0.066) -2.217(0.064)	0.020(0.054) 2.403(0.111) 2.608(0.087) -2.582(0.087)	-0.021(0.045) 2.539(0.094) 2.736(0.082) -2.873(0.179)
0.992(0.027) 0.995(0.026) 0.757(0.027) 0.757(0.000)	0.991(0.025) 0.975(0.039) 0.789(0.014) 0.797(0.000)	0.952(0.065) 0.995(0.044) 0.484(0.160) 0.446(0.033)	0.971(0.030) 0.978(0.015) 0.605(0.045) 0.599(0.026)	0.969(0.025) 0.964(0.020) 0.710(0.028) 0.714(0.015)
0.841(0.031) 0.845 1.667(0.046) 1.372 0.475(0.012) 0.219 0.769(0.024) 337.2	0.784(0.045) 0.882 1.572(0.063) 1.388 0.445(0.017) 0.219 0.775(0.020) 540.4	1.174(0.066) 0.667 2.344(0.133) 1.113 0.750(0.044) 0.199 0.562(0.153) 107.2	1.057(0.045) 0.779 2.102(0.087) 1.239 0.630(0.012) 0.210 0.704(0.023) 108.5	0.924(0.029) 0.828 1.854(0.056) 1.321 0.535(0.013) 0.212 0.741(0.027) 219.6
3.827(0.058) 2.449(0.062) 1.211 1.643(0.040) 1.222(0.020) 0.639(0.021)	3.834(0.033) 2.450(0.067) 1.224 1.665(0.128) 1.233(0.016) 0.639(0.020)	3.566(0.052) 2.686(0.158) 0.869 1.143(0.026) 1.096(0.020) 0.753(0.044)	3.661(0.065) 2.590(0.087) 0.997 1.212(0.032) 1.116(0.014) 0.708(0.036)	3.755(0.046) 2.541(0.049) 1.035 1.295(0.048) 1.143(0.018) 0.677(0.013)
0.868(0.006) 0.729(0.020) 0.249 1.174(0.069) 1.189(0.054) 1.191(0.034)	0.875(0.018) 0.724(0.017) 0.254 1.242(0.100) 1.212(0.029) 1.208(0.016)	0.885(0.025) 0.881(0.080) 0.223 0.948(0.084) 0.959(0.082) 1.011(0.076)	0.907(0.042) 0.794(0.031) 0.223 1.100(0.078) 1.107(0.052) 1.143(0.052)	0.893(0.038) 0.761(0.034) 0.252 1.073(0.064) 1.141(0.037) 1.173(0.031)
0.601(0.037) 12.2	0.636(0.022) 9.4	0.321(0.309) 115.3	0.607(0.092) 43.9	0.648(0.043) 26.2
2.49±1.52 1.25±0.54 8.62±6.04 0.146(0.008)	2.30±1.46 1.42±0.72 10.26±6.67 0.136(0.010)	1.37±0.75 1.00±0.00 5.92±6.08 0.161(0.014)	1.51±0.77 1.00±0.00 6.80±5.53 0.148(0.012)	1.81±1.02 1.02±0.12 6.94±4.23 0.149(0.008)

3) The numerals connected with the double sign indicate the mean and standard deviation of the quantity in question.

Identification	M-1 (400 waves)	M-2	M-3	M-4
Input Data				
m	50.0	50.0	50.0	20.0
n	40.0	40.0	40.0	16.0
$f_{\min} \sim f_{\max}$	0.95~1.25	0.95~1.25	0.95~1.25	0.8~1.8
K	50	50	100	100
nos. of run	10	10	9	5
Distribution of η				
skewness	0.000(0.002)	0.001(0.005)	-0.000(0.002)	-0.000(0.011)
kurtosis	2.901(0.278)	2.768(0.237)	2.840(0.233)	2.923(0.303)
max. η_{\max}	3.087(0.292)	2.970(0.143)	3.037(0.313)	3.051(0.212)
min. η_{\min}	-3.078(0.294)	-2.964(0.151)	-3.028(0.307)	-3.075(0.229)
Nos. of Waves				
ratio of N_0	1.001(0.004)	1.006(0.007)	1.003(0.005)	1.004(0.016)
ratio of N_1	1.001(0.004)	1.006(0.007)	1.002(0.004)	1.002(0.011)
$(\epsilon)_{\text{nos.}}$	0.041(0.042)	0.030(0.046)	0.033(0.047)	0.122(0.069)
$(\epsilon)_{\text{spec.}}$	0.057(0.000)	0.057(0.000)	0.057(0.000)	0.153(0.000)
Crest-to-Trough				
η_{\max}	1.259(0.022)	1.254(0.060)	1.284(0.067)	1.241(0.050)
$\sigma(\eta_{\max})$	0.644	0.610	0.648	0.646
\bar{H}^*	2.517(0.044)	2.570(0.121)	2.567(0.135)	2.483(0.098)
$\sigma(H^*)$	1.285	1.215	1.295	1.272
\bar{T}^*	0.987(0.004)	0.985(0.007)	0.989(0.004)	0.954(0.010)
$\sigma(T^*)$	0.046	0.049	0.050	0.104
$r(H^*, T^*)$	0.021(0.130)	0.039(0.198)	-0.037(0.137)	0.154(0.089)
$H^* - \chi_{20}^2$: median	27.5	27.4	24.0	25.2
Zero-up-Cross				
$H_{1/3}$	3.992(0.107)	3.866(0.133)	4.057(0.184)	3.952(0.134)
\bar{H}	2.521(0.047)	2.505(0.120)	2.567(0.138)	2.504(0.112)
$\sigma(H)$	1.284	1.211	1.295	1.256
$H_{\max}/H_{1/3}$	1.542(0.130)	1.532(0.068)	1.491(0.110)	1.525(0.136)
$H_{1/10}/H_{1/3}$	1.268(0.039)	1.260(0.024)	1.250(0.039)	1.271(0.053)
$\bar{H}/H_{1/3}$	0.632(0.021)	0.649(0.034)	0.633(0.015)	0.634(0.025)
$T_{1/3}$	0.988(0.002)	0.988(0.003)	0.987(0.003)	0.967(0.002)
\bar{T}	0.988(0.004)	0.984(0.008)	0.989(0.004)	0.962(0.015)
$\sigma(T)$	0.058	0.056	0.049	0.100
T_{\max}/\bar{T}	0.994(0.009)	1.000(0.011)	0.996(0.010)	0.996(0.025)
$T_{1/10}/\bar{T}$	1.000(0.001)	1.001(0.011)	0.998(0.008)	0.999(0.026)
$T_{1/3}/\bar{T}$	1.000(0.005)	1.003(0.008)	0.998(0.006)	1.005(0.017)
$r(H, T)$	-0.013(0.169)	0.056(0.204)	-0.038(0.140)	0.117(0.140)
$H - \chi_{10}^2$: median	12.6	15.7	13.7	12.8
Length of Run				
H_{median}	11.58 ± 7.95	10.68 ± 7.19	11.63 ± 9.37	5.01 ± 3.34
$H_{1/3}$	7.33 ± 3.95	5.52 ± 2.84	6.90 ± 3.70	3.51 ± 1.90
$H_{1/3}$ -to- $H_{1/3}$	49.45 ± 36.05	40.64 ± 26.22	40.20 ± 29.32	21.70 ± 11.23
$P(H > H_{1/3})$	0.141(0.010)	0.131(0.016)	0.136(0.015)	0.142(0.021)

Wave Statistics with Spectral Simulation

M-5	M-6	M-7	M-8	M-9
20.0 16.0 0.8~1.8 50 10	10.0 8.0 0.75~3.0 50 10	2.5 2.0 0.2~5.0 50 10	1.25 1.00 0.15~5.0 50 10	0.5 0.4 0~5.0 50 10
0.000(0.001) 2.908(0.303) 3.121(0.280) -3.112(0.316)	0.012(0.016) 2.921(0.312) 3.236(0.264) -3.275(0.366)	-0.015(0.094) 2.869(0.152) 3.227(0.305) -3.545(0.403)	-0.009(0.045) 2.890(0.107) 3.321(0.269) -3.262(0.220)	0.026(0.090) 2.920(0.091) 3.434(0.288) -3.321(0.241)
1.005(0.005) 1.005(0.008) 0.142(0.057) 0.153(0.000)	1.005(0.013) 0.997(0.015) 0.318(0.040) 0.342(0.000)	0.987(0.030) 0.995(0.012) 0.758(0.020) 0.755(0.000)	1.012(0.022) 0.993(0.011) 0.682(0.020) 0.696(0.000)	0.994(0.021) 1.002(0.011) 0.673(0.023) 0.668(0.000)
1.250(0.028) 0.660 2.500(0.057) 1.299 0.952(0.007) 0.104 0.179(0.083) 14.8	1.194(0.030) 0.695 2.389(0.059) 1.306 0.857(0.014) 0.175 0.440(0.063) 19.3	0.832(0.019) 0.853 1.662(0.019) 1.181 0.322(0.004) 0.127 0.638(0.033) 123.7	0.911(0.020) 0.822 1.826(0.024) 1.114 0.278(0.003) 0.088 0.502(0.045) 43.6	0.945(0.017) 0.818 1.886(0.035) 1.084 0.263(0.003) 0.077 0.470(0.035) 43.6
4.002(0.063) 2.520(0.056) 1.281 1.544(0.135) 1.254(0.041) 0.630(0.017) 0.966(0.003) 0.962(0.005) 0.102 0.999(0.020) 1.006(0.012) 1.004(0.006) 0.091(0.082) 7.5	3.927(0.062) 2.514(0.057) 1.236 1.597(0.193) 1.249(0.049) 0.640(0.018) 0.933(0.006) 0.904(0.012) 0.167 1.034(0.033) 1.035(0.018) 1.032(0.016) 0.286(0.068) 8.4	3.666(0.074) 2.350(0.058) 1.133 1.547(0.120) 1.220(0.030) 0.643(0.015) 0.678(0.023) 0.494(0.015) 0.231 1.519(0.334) 1.519(0.072) 1.373(0.033) 0.689(0.039) 10.0	3.537(0.050) 2.321(0.043) 1.061 1.536(0.121) 1.221(0.016) 0.656(0.013) 0.499(0.015) 0.379(0.009) 0.172 1.571(0.610) 1.474(0.097) 1.315(0.034) 0.594(0.048) 11.0	3.498(0.071) 2.357(0.031) 1.006 1.492(0.080) 1.207(0.013) 0.674(0.011) 0.451(0.014) 0.356(0.008) 0.163 1.557(0.663) 1.387(0.103) 1.267(0.047) 0.529(0.058) 16.5
4.94±3.17 2.84±1.44 20.20±13.10 0.141(0.012)	3.10±2.16 1.68±0.92 12.28±8.42 0.140(0.013)	1.93±1.23 1.20±0.54 8.38±5.57 0.145(0.008)	1.92±1.29 1.12±0.37 7.75±4.66 0.143(0.011)	1.97±1.28 1.12±0.36 8.25±4.94 0.138(0.008)

Identification	M_t	N_m
Input Data		
m	5.0	6.0
n	-1.0	2.0
$f_{\min} \sim f_{\max}$	0.3~5.0	0.4~5.0
K	50	50
nos. of run	10	10
Distribution of η		
skewness	-0.001(0.044)	0.054(0.037)
kurtosis	2.914(0.254)	2.922(0.084)
max. η_{\max}	3.393(0.303)	3.482(0.314)
min. η_{\min}	-3.326(0.280)	-3.139(0.273)
Nos. of Waves		
ratio of N_0	1.003(0.027)	0.990(0.022)
ratio of N_1	0.983(0.025)	0.981(0.023)
$(c)_{\text{nos.}}$	0.662(0.022)	0.696(0.022)
$(c)_{\text{spec.}}$	0.680(0.000)	0.704(0.000)
Crest-to-Trough		
$\bar{\eta}_{\max}$	0.947(0.029)	0.910(0.030)
$\sigma(\eta_{\max})$	0.817	0.856
\bar{H}^*	1.885(0.065)	1.832(0.046)
$\sigma(H^*)$	1.405	1.353
\bar{T}^*	0.591(0.016)	0.523(0.012)
$\sigma(T^*)$	0.237	0.209
$r(H^*, T^*)$	0.757(0.025)	0.718(0.026)
$H^* - \chi_{20}^2$: median	196.4	190.9
Zero-up-Cross		
$H_{1/3}$	3.840(0.057)	3.821(0.059)
\bar{H}	2.459(0.066)	2.466(0.047)
$\sigma(H)$	1.227	1.182
$\bar{H}_{\max}/H_{1/3}$	1.636(0.150)	1.575(0.098)
$H_{1/10}/H_{1/3}$	1.240(0.034)	1.228(0.022)
$\bar{H}/H_{1/3}$	0.641(0.024)	0.648(0.014)
$T_{1/3}$	0.907(0.007)	0.879(0.014)
\bar{T}	0.788(0.019)	0.729(0.017)
$\sigma(T)$	0.234	0.251
T_{\max}/\bar{T}	1.121(0.092)	1.215(0.121)
$T_{1/10}/\bar{T}$	1.146(0.045)	1.224(0.060)
$T_{1/3}/\bar{T}$	1.152(0.029)	1.205(0.021)
$r(H, T)$	0.581(0.045)	0.592(0.052)
$H - \chi_{10}^2$: median	12.4	10.2
Length of Run		
H_{median}	2.62±1.79	2.25±1.55
$H_{1/3}$	1.46±0.68	1.25±0.52
$H_{1/3}$ -to- $H_{1/3}$	11.03±6.42	8.93±5.62
$P(H > H_{1/3})$	0.131(0.010)	0.137(0.011)

Wave Statistics with Spectral Simulation

Identification	D-1	D-2	D-3	D-4
Input Data				
m, n	5.0, 4.0	5.0, 4.0	5.0, 4.0	5.0, 4.0
m', n'	10.0, 8.0	10.0, 8.0	10.0, 8.0	10.0, 8.0
α	0.2	1.0	5.0	25.0
$f_{\min} \sim f_{\max}, \beta$	0.3~3.0, 0.4	0.3~3.0, 0.4	0.3~3.0, 0.4	0.3~3.0, 0.4
K	60	60	60	60
nos. of run	5	5	5	5
Distribution of η				
skewness	-0.032(0.054)	0.038(0.067)	-0.021(0.053)	0.032(0.021)
kurtosis	2.874(0.223)	2.899(0.069)	2.940(0.088)	2.878(0.054)
max. η_{\max}	3.277(0.549)	3.495(0.305)	3.271(0.128)	3.087(0.138)
min. η_{\min}	-3.272(0.286)	-3.084(0.216)	-3.422(0.451)	-3.490(0.176)
Nos. of Waves				
ratio of N_0	0.984(0.011)	1.000(0.007)	1.001(0.027)	1.002(0.045)
ratio of N_1	0.981(0.011)	0.993(0.011)	0.990(0.017)	0.985(0.021)
$(c)_{\text{nos.}}$	0.599(0.016)	0.646(0.010)	0.770(0.018)	0.855(0.014)
$(c)_{\text{spec.}}$	0.603(0.000)	0.652(0.001)	0.767(0.001)	0.861(0.000)
Crest-to-Trough				
η_{\max}	1.031(0.021)	0.959(0.019)	0.816(0.021)	0.659(0.025)
$\sigma(\bar{\eta}_{\max})$	0.778	0.822	0.871	0.934
\bar{H}^*	2.054(0.030)	1.937(0.029)	1.633(0.022)	1.306(0.041)
$\sigma(H^*)$	1.309	1.249	1.164	1.178
\bar{T}^*	0.632(0.005)	0.629(0.007)	0.651(0.008)	0.763(0.018)
$\sigma(T^*)$	0.216	0.212	0.232	0.393
$r(H^*, T^*)$	0.640(0.009)	0.634(0.037)	0.618(0.018)	0.681(0.035)
$H^* - \chi_{20}^2$: median	72.5	79.9	139.5	288.8
Zero-up-Cross				
$H_{1/3}$	3.795(0.043)	3.697(0.032)	3.624(0.056)	3.833(0.075)
\bar{H}	2.500(0.033)	2.443(0.030)	2.342(0.059)	2.262(0.090)
$\sigma(H)$	1.156	1.105	1.112	1.328
$H_{\max}/H_{1/3}$	1.594(0.199)	1.564(0.107)	1.558(0.116)	1.650(0.116)
$H_{1/10}/H_{1/3}$	1.227(0.037)	1.216(0.018)	1.229(0.012)	1.273(0.023)
$\bar{H}/H_{1/3}$	0.659(0.014)	0.661(0.007)	0.646(0.015)	0.590(0.016)
$T_{1/3}$	0.899(0.014)	0.966(0.023)	1.407(0.046)	2.217(0.024)
\bar{T}	0.788(0.009)	0.822(0.007)	1.018(0.029)	1.467(0.065)
$\sigma(T)$	0.248	0.302	0.499	0.731
T_{\max}/\bar{T}	1.029(0.120)	1.049(0.062)	1.905(0.384)	1.555(0.121)
$T_{1/10}/\bar{T}$	1.095(0.040)	1.145(0.048)	1.653(0.127)	1.558(0.077)
$T_{1/3}/\bar{T}$	1.122(0.041)	1.175(0.027)	1.382(0.012)	1.515(0.066)
$r(H, T)$	0.505(0.044)	0.498(0.036)	0.679(0.031)	0.818(0.020)
$H - \chi_{10}^2$: median	11.4	14.6	15.6	17.1
Length of Run				
H_{median}	2.41 ± 1.71	2.22 ± 1.76	1.97 ± 1.55	2.67 ± 2.09
$H_{1/3}$	1.24 ± 0.45	1.21 ± 0.45	1.23 ± 0.58	1.82 ± 1.11
$H_{1/3}$ -to- $H_{1/3}$	9.68 ± 6.44	8.05 ± 6.16	8.80 ± 6.83	12.28 ± 8.64
$P(H > H_{1/3})$	0.130(0.013)	0.149(0.007)	0.138(0.006)	0.145(0.014)